Article:
Kirk, J.A., Gebhart, D., Buckley, A.M. et al. (2017) New Class of Precision Antimicrobials Redefines Role of Clostridium difficile S-layer in Virulence and Viability. Science Translational Medicine, 9 (406). eaah6813. ISSN: 1946-6234

https://doi.org/10.1126/scitranslmed.aah6813

New Class of Precision Antimicrobials Redefines Role of *Clostridium difficile* S-layer in Virulence and Viability

Joseph A. Kirk[1], Dana Gebhart[2], Anthony M. Buckley[3], Stephen Lok[2], Dean Scholl[2], Gillian R. Douce[3], Gregory R. Govoni[2*], Robert P. Fagan[1*]

[1] Krebs Institute, Department of Molecular Biology and Biotechnology University of Sheffield, Sheffield S10 2TN, UK.

[2] AvidBiotics Corp. South San Francisco, California, USA.

[3] Institute of Infection, Immunity and Inflammation, College of Medical, Veterinary & Life Sciences, University of Glasgow, Glasgow G12 8TA, UK.

*To whom correspondence should be addressed: Gregory R. Govoni: ggovons@gmail.com; Robert P. Fagan: r.fagan@sheffield.ac.uk

One Sentence Summary:

We have constructed a series of antimicrobial agents called Avidocin-CDs that specifically bind to the highly polymorphic S-layer and kill *C. difficile*; rare escape mutants lacked Surface layer protein A (SlpA) and exhibited severe phenotypic defects that fully compromised virulence without affecting colonization of the hamster gut.

Abstract:

Avidocin-CDs are a new class of precision bactericidal agents that do not damage resident gut microbiota and are unlikely to promote the spread of antibiotic resistance. The precision killing properties result from the fusion of bacteriophage receptor binding proteins (RBPs) to a lethal contractile scaffold from an R-type bacteriocin. We recently described the prototypic Avidocin-CD, Av-CD291.2, that specifically kills *C. difficile* ribotype 027 strains and prevents

colonization of mice. We have since selected two rare Av-CD291.2 resistant mutants of strain R20291 (RT027; S-layer cassette type-4, SCLT-4). These mutants have distinct point mutations in the *slpA* gene that result in an S-layer null phenotype. Reversion of the mutations to wild-type restored normal SLCT-4 S-layer formation and Av-CD291.2 sensitivity; however, complementation with other SCLT alleles did not restore Av-CD291.2 sensitivity despite restoring S-layer formation. Using newly identified phage RBPs, we constructed a panel of new Avidocin-CDs that kill *C. difficile* isolates in an SLCT-dependent manner, confirming the S-layer as the receptor in every case. In addition to bacteriophage adsorption, characterization of the S-layer null mutant also uncovered important roles for SlpA in sporulation, resistance to lysozyme and LL-37, and toxin production. Surprisingly, the S-layer-null mutant was found to persist in the hamster gut despite its completely attenuated virulence. Avidocin-CDs have significant therapeutic potential for the treatment and prevention of *C. difficile* Infection (CDI) given their exquisite specificity for the pathogen. Furthermore, the emergence of resistance forces mutants to trade virulence for continued viability and, therefore, greatly reduce their potential clinical impact.

Introduction

New antibacterial agents are needed to counteract the impending loss of effective treatment options for multi-drug resistant bacteria. Furthering this need is the realization that dysbiosis caused by broad-spectrum antibiotic use contributes to the prevalence of diseases/disorders such as inflammatory bowel disease, obesity and gastrointestinal infections (*1*). Strategies to overcome these threats include use of narrow spectrum or precision agents and the design of drugs that target virulence instead of *in vitro* viability (*2, 3*). One pathogen for which alternative treatment approaches are needed is *C. difficile*. This spore-forming, obligate anaerobe is the leading cause of nosocomial infections worldwide. Approximately 450,000 cases and 29,000 deaths each year are attributed to this pathogen in the US alone (*4*). As a result, the Centers for Disease Control and Prevention has identified *C. difficile* as an urgent threat to human health (*5*). This opportunistic pathogen exploits a reduction in gut microbiota diversity that often follows broad spectrum antibiotic use to proliferate, release toxins, and cause life-threatening colitis (*6*). Although the toxins have been studied in great detail, other aspects of *C. difficile* virulence, including colonization of the gut, are not well understood (*6*). The *C. difficile* cell surface is covered by a paracrystalline surface layer (S-layer) largely comprised of SlpA and sparsely interspersed by 28 related cell wall proteins (*7*). The S-layer precursor SlpA is proteolytically processed on the cell surface to generate the Low and High Molecular Weight S-layer Proteins (LMW and HMW SLPs). The SLPs interact with high-affinity to form a heterodimer, the basic unit of the mature S-layer (*8*). The *slpA* gene is located within a highly variable S-layer cassette consisting of 5 genes; 13 distinct S-layer cassette types (SLCTs) have been described to date (*9*). The variation that defines individual cassette types is largely confined to the LMW SLP-encoding region of *slpA* (*4*). The HMW SLP region is highly conserved and includes the cell

wall binding motifs that anchor the S-layer to the cell wall (*10*). The S-layer and several associated cell wall proteins have been implicated in colonization of host tissues (*7*) and in stimulation of the host immune response via TLR4 signaling (*11*).

Whereas *C. difficile* is not significantly resistant to the frontline antibiotics used to treat CDIs (vancomycin, metronidazole and fidaxomicin), the use of these antibiotics causes further disruption of the resident microbiota leading to frequent CDI relapse (*6*). To be safe and effective, new agents to treat and prevent CDIs must not harm the diverse gut microbiota and the colonization resistance it provides. Avidocin-CDs represent one such potential agent (*12*). These bactericidal proteins are genetically modified versions of natural R-type bacteriocins (a.k.a. diffocins) produced by *C. difficile* to kill competing *C. difficile* strains (*13*). Diffocins resemble *myoviridae* phage tails and consist of a contractile sheath, nanotube core, baseplate and tail fiber structures. However, instead of delivering DNA across the bacterial membrane as does a bacteriophage, R-type bacteriocins function as killing machines by injecting a nanotube core through the bacterial cell envelope and creating a small pore that dissipates the cell's membrane potential (*14*). Killing specificity is determined by the receptor binding proteins (RBPs) located at the tail fiber tips that trigger sheath contraction upon binding with a cognate receptor on the bacterial cell surface. Genetic replacement or fusion of the RBP gene with homologues from other strains or RBP sources (i.e. *C. difficile* bacteriophages and prophage insertions) make it possible to retarget killing (*12, 15-17*). These modified bacteriocins are known as Avidocin-CDs. An Avidocin-CD prototype, Av-CD291.2, constructed with a bacteriophage RBP identified within a prophage insertion was found to be more stable than the natural parent diffocin. Av-CD291.2 had a modified killing spectrum that included all hypervirulent RT027 *C. difficile* strains tested, blocked *C. difficile* colonization in a mouse model of spore transmission and did

not disrupt the resident gut microbiota (*12*). These properties encourage the further development of Avidocin-CDs as oral human therapeutics.

Here we further characterize the Av-CD291.2 mechanism of action and describe an expanded panel of Avidocin-CDs that cover all clinically relevant *C. difficile* strain types using newly identified bacteriophage RBPs. Rare resistant mutants were isolated *in vitro* under Av-CD291.2 selection. Analysis of these mutants enabled the identification of SlpA as the cell surface receptor for all tested Avidocin-CDs and, by extension, the corresponding bacteriophage and prophage RBP-sources. We also identified previously unsuspected roles for SlpA in sporulation, resistance to lysozyme and the natural anti-microbial peptide LL-37, toxin production and virulence. Surprisingly, despite their complete attenuation of virulence, resistant mutants could colonize and persist in the hamster gut for the duration of a 14-day study. These findings imply that antimicrobial agents that force pathogens to trade virulence for continued viability would have clear clinical advantages should resistance emerge during treatment.

Results

Av-CD291.2-resistant mutants lack an S-layer

Resistance to any antimicrobial agent can occur and be exploited to understand its mode of action. We isolated two spontaneous mutants of *C. difficile* strain R20291 (ribotype 027) that were resistant to killing by Av-CD291.2. These mutants appeared at a frequency of $< 1 \times 10^{-9}$ and were found to encode independent point mutations in the *slpA* gene (Fig. 1A). Both mutations were predicted to truncate SlpA at a site N-terminal to the post-translational cleavage site and, thereby, prevent formation of an S-layer. Both FM2.5 and FM2.6 lacked detectable cell surface S-layer protein subunits as predicted but still expressed minor cell wall proteins including Cwp2 and Cwp6 (Fig. 1B). These mutations did not affect the growth rate of the bacteria *in vitro* (Fig. S4B); however, FM2.5 displayed a slight, but statistically significant earlier entry into stationary phase (maximum OD_{600nm}: FM2.5 = 2.2; R20291 = 3.2, p = 0.000012). We attempted to complement the FM2.5 and FM2.6 mutations with a plasmid-borne wild-type R20291 *slpA*; however, unexpected homologous recombination restored the wild type *slpA* gene to the chromosome (Fig. S1). Accordingly, we created genetically identifiable recombinants "watermarked" with synonymous substitutions in the R20291 *slpA* allele (Fig. 1A). The resulting strains, FM2.5RW and FM2.6RW, were found to have LMW and HMW SLPs on their surface (Fig. 1B) and regained sensitivity to Av-CD291.2 (Fig. 1C and D). These results confirmed that an intact S-layer is required for Av-CD291.2 killing but did not determine whether SlpA itself or a protein dependent on the S-layer for surface localization was the receptor for Av-CD291.2. To address this question, *slpA* alleles from the most common non-R20291 SLCTs were individually cloned into an inducible expression plasmid and transferred into the S-layer deficient FM2.5 (Fig. 1E). Each resulting strain expressed the expected LMW

and HMW SLPs on the cell surface, indicative of S-layer formation (*9*), but did not regain sensitivity to Av-CD291.2, thus, ruling out the possibility that the simple formation of an S-layer was responsible for sensitivity to Av-CD291.2. To address whether Av-CD291.2 directly interacts with SLCT-4 SlpA, plasmids encoding SlpA from 8 different SLCTs were introduced into the non-isogenic laboratory strain 630 (SLCT-7; ribotype 012), which is insensitive to Av-CD291.2 (Table S1). In this fully S-layer competent SLCT-7 wild type strain, only induction of SLCT-4 SlpA was sufficient to confer sensitivity to Av-CD291.2 (Fig. S3). Moreover, the degree of sensitivity was dependent on the level of induction with only 10 ng/mL of inducer required (Fig. S3A). Taken together these observations clearly demonstrate that the SLCT-4 variant of SlpA is the cell surface target of Av-CD291.2.

Sensitivity to all Avidocin-CDs is slpA allele-specific

These observations suggested that each variant of SlpA may serve as a specific receptor for additional *C. difficile* bacteriophage RBPs. In an attempt to expand Avidocin-CD coverage beyond SLCT-4, we constructed ten new Avidocin-CDs using predicted bacteriophage RBPs mined from the genome sequences of *C. difficile* clinical isolates or newly isolated bacteriophages (Table S1). Source strains for RBP sequences were chosen based on their SLCT since strain typing information for the RBP source often correlates with sensitivity to the corresponding Avidocin (*e.g.* ribotype 027 and sensitivity to Av-CD291.2; SLCT-1 of phi-147 propagating strain and sensitivity to Av-CD147.1) (*12, 15, 16*). Preparations of Diffocin-4 (scaffold for all Avidocin-CDs), Av-CD291.2, and each of the new Avidocin-CDs were tested for killing activity on a panel of 62 *C. difficile* isolates containing all 13 known SLCTs and a newly identified 14th SLCT (Fig. S2). Only two strains, representing SLCTs 3 and 5, were not killed by a single Avidocin-CD (Fig S2); otherwise, every isolate from all 12 other SLCTs was

killed by at least one Avidocin-CD. A near perfect correlation was observed between a strain's SLCT and its sensitivity to each of the Avidocin-CDs. The only exceptions were SLCT-2 isolates with Av-CD027.2 and Av-CD685.1. A strong correlation was also observed between ribotype and sensitivity to a particular Avidocin-CD since all ribotypes in the panel, except 012, 014 and 015, were found to associate exclusively with a single SLCT. Similar correlations with strain sensitivity and SLCT or ribotype were not observed for killing with Diffocin-4, suggesting this natural R-type bacteriocin binds to *C. difficile* via another receptor.

Having made these observations, we wanted to determine if sensitivity to specific Avidocin-CDs was directly dependent upon the variant of SlpA present. The panel of isogenic FM2.5 strains complemented with *slpA* alleles from the 10 most common SLCTs was tested for sensitivity to a panel of the most potent Avidocin-CDs (Fig. 2). The corresponding parental strains from which the *slpA* alleles were obtained were used as controls. Each complemented strain became sensitive to the same Avidocin-CDs as the parental strain. To confirm that this engineered sensitivity did not result from altered cell surface architecture, an analogous experiment was performed in a second panel of isogenic strains created when plasmids encoding SlpAs from 8 SLCTs were introduced into the S-layer competent strain 630 (Fig. S3B and C). As before, the spectrum of killing was identical to that of the parental strains from which the *slpA* alleles were obtained. These data conclusively demonstrate that the polymorphic SlpA acts as the binding receptor for each of the Avidocin-CDs tested and, therefore, the corresponding bacteriophage RBPs.

S-layer null mutants are abnormally sensitive to innate immune effectors

Bacterial S-layers serve many critical cellular functions (*7*). Given its location on the cell surface, the S-layer has been proposed to act as a molecular sieve to selectively limit exposure of

the underlying cell envelope to large biomolecules such as the innate immune effector lysozyme (*18*). Until now, analysis of *C. difficile* S-layer function has been hampered by an inability to isolate *slpA*-deficient mutants (*19*). While *C. difficile* is highly resistant to killing by this enzyme, resistance has been attributed to extensive peptidoglycan deacetylation (*20*). To determine if the S-layer also plays a role in lysozyme resistance, we treated exponentially growing bacteria with a high concentration of lysozyme (500 μg/ml) and monitored the effects on growth (Fig. 3A). Upon addition of lysozyme an immediate decrease in optical density consistent with cell lysis, followed by slower growth, was observed for the S-layer mutant FM2.5. In contrast, R20291 and FM2.5RW displayed only a transient decrease in growth rate, consistent with natural resistance. Having confirmed a role for the S-layer in lysozyme resistance, we then tested for resistance to the human cathelicidin antimicrobial peptide LL-37 to determine if S-layer-mediated resistance extended to other innate immune effectors (Fig. 3B). LL-37 is found at mucosal surfaces at concentrations of up to 5 μg/ml in normal conditions with further expression induced in response to infection (*21*). Treatment with 5 μg/ml of LL-37 completely killed exponentially growing cultures of the S-layer mutant FM2.5; whereas, the same treatment caused only a slight reduction in growth rates for R20291 and FM2.5RW. Taken together, these data demonstrate a role for the S-layer in resistance to both lysozyme and LL-37.

S-layer null mutants display severe sporulation defects

It was noted that the S-layer mutant strains survived poorly in the standard charcoal medium used to transport *C. difficile* strains. The ability of *C. difficile* to survive in the environment and be transmitted to new hosts is reliant on the bacterium's ability to produce a heat and chemical-resistant spore (*22*). We analyzed sporulation efficiency by measuring the numbers of heat-resistant spores as a percentage of total viable CFUs over 5 days (Fig. S4A).

Spore production by wild type R20291 and FM2.5RW cultures was reproducible and equivalent and represented 73 and 85% of total viable counts on day 5, respectively (Fig. 3C). In contrast, spore production by FM2.5 was significantly lower (p = <0.00001). Spores only represented 4.3% of total viable counts on day 5, which is a 17-20-fold reduction compared to R20291 and FM2.5RW. These observed differences in FM2.5 spore formation were not due to an inability to germinate efficiently (Fig. 3D). When the bile salt germinant taurocholate was added to purified spore preparations, the speed and efficiency of germination initiation for FM2.5 spores was indistinguishable from that of R20291 and FM2.5RW. Analysis of bacterial cultures by phase contrast microscopy also pointed to a reduction in sporulation efficiency (Fig. S4C and D), as 5.2-fold fewer phase bright spores were observed in cultures of FM2.5 (FM2.5, 8.7% vs R20291, 44.9%; FM2.5RW, 45.4%). Interestingly, we noted a discrepancy between the magnitudes of the sporulation defect determined microscopically (5.2-fold less than R20291) compared with direct counting of viable spore CFUs (20-fold less than R20291). This suggests that many of the microscopically counted spores were nonviable following the 65°C heat treatment required to differentiate spores from vegetative cell CFUs. To test the FM2.5 spores for possible stress resistance defects, we exposed the cultures to a harsher heat treatment (75°C for 30 min). The 75°C heat treatment further reduced FM2.5 spore viability 33-fold compared with the standard 65°C (Fig. 3C). The same treatment only reduced spore viability by 1.5-fold for R20291 and 2-fold for FM2.5RW. Collectively, these data indicate that the production and quality of the infectious spores are severely impaired by the loss of the S-layer.

Transmission electron microscopy was employed to identify potential morphological changes associated with these defects (Fig. S5). In FM2.5 cultures we observed spores with disorganized material loosely attached to the electron-dense core that lacked discernible, well-

organized protein coat layers (*23*)(Fig. S5A). To determine if these unusual spore morphologies were responsible for the observed thermal sensitivity, we repeated these analyses with spores purified on a Histodenz gradient. Following purification, spores of FM2.5 were morphologically indistinguishable from those of R20291 and FM2.5RW (Fig. S5C). Surprisingly, purified FM2.5 spores still displayed increased thermal sensitivity. A75°C heat treatment reduced FM2.5 spore viability 37.1-fold compared to 10- and 18.1-fold for R20291 and FM2.5RW respectively (Fig. S5B). Several distinct biochemical and structural features of the spore, including the concentric cortex peptidoglycan and protein layers and core dehydration, have been independently linked to heat resistance (*24-26*). Minor defects in any of these features could explain the observed thermal sensitivity of FM2.5 spores.

S-layer null mutants are completely avirulent despite persistent gut colonization

We tested the ability of the S-layer mutant FM2.5 to cause disease in the Golden Syrian hamster model of acute CDI. As expected, all animals inoculated with FM2.5RW behaved similarly to animals inoculated with the wild type R20291 strain and succumbed to *C. difficile* infection within 102 h of infection, with mean times to cull for R20291 and FM2.5RW of 67 h 36 min and 57 h 19 min, respectively ($p = 0.52$, Fig. 4A). Both groups of hamsters showed typical signs of disease including wet tail and drop in body temperature at experimental endpoint. In contrast, all animals inoculated with FM2.5 displayed no signs of disease and survived for the duration of the 14-day study ($p = 0.0018$; FM2.5 vs R20291, Fig. 4A). Very few described mutations located outside of the PaLoc locus have resulted in complete avirulence in this model (*27*). Surprisingly, the lack of virulence was not due to a colonization defect. FM2.5 was capable of persistent colonization; CFUs in the caecum and colon at the end of study (14 days) were not statistically different to those observed for R20291 and FM2.5RW in the same

tissues taken at experimental endpoint some 10 days earlier (Fig. 4B). Toxin measurements from gut contents 14 days after inoculation with FM2.5 showed dramatic reductions in both toxin A or B activity compared to samples taken from hamsters that succumbed to infection with either the R20291or FM2.5RW (Fig. 4C and 4D).

***S-layer null mutants lack toxin production* in vitro**

Given the avirulence and low toxin activity observed in animals, we assayed the FM2.5 and control strains for toxin production *in vitro* (Fig. 4E). Toxin B was used as an indicator for both toxins since they are coordinately expressed and released (*6*). As expected, both R20291 and FM2.5RW produced toxin upon entry into stationary phase. A small amount of Toxin B was detected intracellularly at 24 hours; thereafter, Toxin B was exclusively detected in the culture supernatant. Cultures of FM2.5 produced less Toxin B at all time-points, consistent with *in vivo* observations.

Discussion

The bactericidal properties of Avidocin-CDs bode well for the clinical application of this new class of antimicrobial agents for combating CDI. Previous studies demonstrated that killing by the prototypic Avidocin-CD, Av-CD291.2, was highly specific for BI/NAP1/027-type strains and did not detectably alter the resident gut microbiota in mice (*12*). For production purposes fermentation of genetically modified *B. subtilis* expressing these agents is similar to many established industrial processes and scalable to thousands of liters. We selected, isolated and characterized rare *C. difficile* mutants resistant to Av-CD291.2 to better understand its mechanism of action. In the process we discovered the Avidocin-CD binding receptor, the *C. difficile* S-layer protein SlpA. Indeed, our 10 new Avidocin-CDs were all found to target variants of SlpA associated with different SLCTs. Given that the great majority of the sequence variation in SlpA is found within the surface exposed LMW subunit (*9*), this relationship between SLCT and Avidocin-CD sensitivity strongly suggests that the LMW SLP is the binding site for all the studied Avidocin-CDs. Further, it indirectly identifies this portion of the SlpA as the binding receptor for many *C. difficile* myophages since each Avidocin-CDs is constructed with a different bacteriophage-derived RBP. These findings help explain the limited host ranges observed for many *C. difficile* myophages (*28, 29*). It also suggests that antigenic variation observed between SLCTs may not be due to immune escape as previously proposed (*9*) but rather due to a molecular arms race between bacteria and bacteriophages. *C. difficile* is under selective pressure to change the bacteriophage receptor, which in turn puts selective pressure on the bacteriophages to evolve new RBPs.

Interestingly, patterns of strain sensitivity to each Avidocin-CD indicate killing was much broader than the parental bacteriophage's host range (Fig. S2 and S7). A possible

explanation for this observation is that a typical bacteriophage infection cycle is a 7-step process: attachment, genome injection, replication, transcription, translation, assembly and lysis. Bacteria can become resistant to a bacteriophage by blocking any stage of the infection cycle. For example, CRISPR-Cas or restriction-modification systems that prevent phage DNA from replicating (*30*). In contrast, Avidocin-CD killing is a 2-step process: attachment to the target bacterium followed by killing via creation of a small pore that dissipates the target bacterium's membrane potential, importantly, without lysis or release of macromolecules such as exotoxin from the cytoplasm (Fig. S6). As observed with other Avidocins and R-type bacteriocins (*16, 31*), selected Avidocin-CD resistant mutants survived due to mutations that caused the loss or modification of the SlpA binding receptor and not due to mutations that directly disrupted the killing mechanism, such as improper pore formation, or caused proteolytic cleavage of the agent. The bias towards receptor mutations suggests the Avidocin-CD killing mechanism is simple and robust.

Modification of the binding receptor to avoid Avidocin-CD killing either through missense mutations or S-layer switching, as evidenced by the random association between clades and SLCTs (*9*), could also theoretically lead to resistance. While sequence variations between *slpA* alleles within each SLCT indicate missense mutations do occur (*9*), our findings suggest resistance due to this type of modification is unlikely since the bacteriophage RBPs used to construct the Avidocin-CDs have already evolved to counter this mode of potential escape. For instance, both Av-CD684.1 and Av-CD685.1 kill every SLCT-7 strain tested despite sequence identities between SLCT-7 SlpAs as low as 81% (Fig. S8). As for the emergence of resistance via horizontal transfer of the S-layer cassette, the administration of a cocktail of Avidocin-CDs that kill all the common SLCTs would make successful resistance via S-layer switching

extremely unlikely. It appears that the only likely means of resistance to all the Avidocin-CDs is through complete loss of SlpA, as observed for resistance to Av-CD291.2. As a consequence the observed phenotypes for FM2.5 are germane to all likely Avidocin-CD-resistant mutants.

For a precision medicine agent to be successful, knowing the molecular target, in this case the binding receptor, is vital in designing accurate diagnostics to guide treatment decisions. If Avidocin-CDs were to be administered individually, a diagnostic determining SLCT of infecting *C. difficile* would be highly accurate for informing Avidocin-CD treatment decisions. However, an increase in the prevalence of hybrid cassettes, as found in ribotype 078 strains (*9*), would decrease the accuracy for this typing method. Strain ribotyping could also be employed to avoid development of new diagnostics, but predicting sensitivity to a particular Avidocin-CD may be challenging as ribotypes are not consistently linked to a single SLCT (*i.e.* 012, 014, and 015, as noted above). SlpA-typing would provide the most accurate diagnostic as well as prove more illuminating than ribotyping since SlpA is directly related to the physiology of *C. difficile*, whereas, ribotyping detects physiologically inconsequential ribosomal RNA gene polymorphisms. It may also be possible to administer a cocktail of 5-6 Avidocin-CDs that target 12 of the 14 *C. difficile* SLCTs. If such a cocktail of Avidocin-CDs were to be administered, a point of care diagnostic would only need to detect the presence of *C. difficile* to guide treatment decisions.

The strong selective pressure afforded by Av-CD291.2 allowed isolation of the first spontaneous *C. difficile* S-layer null mutants. In addition to enabling identification of the Avidocin-CD cell surface receptor, these mutants also provide an unprecedented opportunity to study S-layer function (Fig. 5). Given the ubiquity of S-layers in both Bacteria and Archaea, including many pathogenic species, surprisingly little is known about their function. It has been

suggested that the S-layer could act as a molecular sieve to exclude certain large biomolecules from the cell envelope (*18*); however, this has not been confirmed in live cells. We have demonstrated that an intact S-layer is required for resistance to two components of the innate immunity system, lysozyme and the antimicrobial peptide LL-37. Assembled S-layers are highly symmetrical with regular repeating pores. The size of the pores in the *C. difficile* S-layer is not yet known but in other species pore sizes of between 2 and 6 nm have been reported. A pore size of 2 nm could conceivably exclude the16 kDa globular protein lysozyme but a small peptide such as LL-37 would experience no such steric hindrance. It is possible that charged surfaces on the assembled S-layer serve to sequester the cationic peptide away from the cell envelope in a manner analogous to capsular polysaccharides (*32*). Our data has identified other pleiotropic functions for the *C. difficile* S-layer. It is clear that the S-layer is the cell surface receptor for all of the Avidocin-CDs described here and, by extension, the receptor for the bacteriophages from which the RBP-encoding genes were cloned. Although a Bacillus bacteriophage has been found to bind S-layer protein Sap (*33*), this is the first time a receptor for a *C. difficile* bacteriophage has been identified. Furthermore, our data imply that S-layer recognition is a common feature of bacteriophages that infect this species.

Surprisingly, the S-layer mutant also displayed severe sporulation defects, with fewer and morphologically defective spores produced. Despite a number of well-studied spore-forming organisms producing S-layers, including *B. anthracis* (*33*), S-layer biogenesis has not been reported previously to affect sporulation. There is currently no evidence to suggest that the SLPs are a structural part of the mature spore and the mechanisms by which the S-layer can influence sporulation are currently unknown. However, this observation has serious ramifications for the ability of an Avidocin-CD-resistant, S-layer defective mutant to survive and be transmitted to

other hosts. The spore is an absolute requirement for *C. difficile* survival in the aerobic environment and is critical for transmission (*22*). In addition to sporulation defects, the S-layer mutant was also found to produce less toxin *in vitro*. Interestingly, there have been previous suggestions of feedback between sporulation and the complex regulatory network controlling toxin production (*22*). Although the mechanism by which these processes are affected in SlpA null mutants is far from clear, it is possible that the S-layer feeds into a point of crosstalk between regulation of virulence and transmission. Given the poor toxin production and other diverse phenotypes identified for the S-layer mutant, it is probably not surprising that the mutant was entirely avirulent in the hamster model of acute infection. What did come as a surprise, however, was the ability of the S-layer mutant to stably colonize and persist in the hamster gut for the 14-day duration of the experiment. Previous reports have pointed to a role for the S-layer in epithelial cell adhesion; however, these earlier studies were performed without access to an *slpA*-defective strain (*34*). The S-layer defective mutants and isogenic controls expressing the SLCT-specific *slpA* alleles provide the ideal controls to test these conflicting findings and better define the effect SlpA type has on these functions.

There are several study limitations that should be considered when evaluating the data presented. The activity of each new Avidocin-CD was observed *in vitro* and needs to be confirmed in an animal treatment model, as done for Av-CD291.2. Similarly, the exquisite specificity of each agent for distinct *C. difficile* SLCTs also needs be tested *in vivo* to confirm that treatment with these agents will not alter the diversity of the gut microbiota. The avirulent phenotype and long-term persistence of the Avidocin-CD-resistant *slpA* mutants in the hamster model should also be confirmed in other animal species. Finally, the implications of the mutants'

observed sporulation defects on transmission and the spread of resistance remain to be tested *in vivo*. In all cases, we do not anticipate different outcomes from those described here.

After accounting for these limitations, analysis of the data clearly demonstrates that acquisition of Avidocin-CD resistance results in loss of toxin production and complete loss of virulence. Virulence factors make attractive targets for new antimicrobials as they tend to be species-specific, and emergence of resistance is likely to reduce virulence. The ability of the S-layer mutant to stably colonize the gut in the absence of clinical disease reveals that the *in vivo* lifestyle of the organism is independent of toxin production and virulence. The prevalence of non-toxigenic, avirulent *C. difficile* strains in the general population (*35*) supports this hypothesis. As a result, we predict that there will be no competing selective pressure to restore virulence in the context of Avidocin-CD resistance.

In summary, we have developed and characterized multiple new Avidocin-CDs, providing crucial insights into their potential advantages in the clinic. The precise killing activity of Avidocin-CDs makes them attractive agents for both treatment and prevention since they can be administered to patients without altering the diversity of the complex gut microbiota. In addition, when resistance does emerge, Avidocin-CDs force the pathogen to sacrifice virulence for viability - making the potential clinical impact of resistance inconsequential.

Materials and Methods

Study design

The objective of this study was to characterize a panel of Avidocin-CDs, anti-bacterial protein complexes constructed to specifically target and kill *C. difficile*. During these experiments, the isolation of Avidocin-CD resistant *slpA* mutants allowed detailed analysis of S-layer function for the first time. Starting from the prototypic Av-CD291.2 (*12*) we constructed a panel of new Avidocin-CDs using bacteriophage RBPs we identified. Each new Avidocin-CD displayed a unique spectrum of killing activity with a strong correlation to SLCT. Sensitization of two insensitive *C. difficile* strains by heterologous expression of a cognate SLCT SlpA alone allowed identification of the S-layer as the receptor for all described Avidocin-CDs. Analysis of the *slpA* mutant identified previously unsuspected *in vitro* roles for the S-layer in resistance to the immune effectors lysozyme and LL-37, and in the production of mature heat-resistant spores. Finally, use of the Golden Syrian hamster model of acute infection demonstrated that the *slpA* mutant was entirely avirulent despite persistent infection. Greatly reduced toxin activity was detected in intestinal contents from animals colonized with the *slpA* mutant and this observation was supported by identification of a toxin production defect *in vitro*. The design and execution of these animal experiments is described in detail in Supplementary Methods.

Strains, bacteriophage and culture conditions.

Bacterial strains used in this study are described in Figure S2. DNA oligonucleotides are described in Table S2. *E. coli* strains were routinely grown in LB broth and on LB agar (VWR). *C. difficile* strains were routinely grown under anaerobic conditions on BHI or BHI-S agar and in TY broth (*36*) except where otherwise stated. Cultures were supplemented with chloramphenicol

(15 μg/ml), thiamphenicol (15 μg/ml) or anhydrotetracycline (20 ng/ml) as required. *C. difficile* SLCTs were determined by analyzing the nucleotide sequence of the *slpA* gene. When necessary, the *slpA* gene was sequenced using oligonucleotide primers previously described (*37, 38*) or primers 023-F and 023_010-R or 014+++-F and 014_002+-R (nucleotide sequences - Table S2). The variable region of strain 19142 (ribotype 046) *slpA* gene did not display high sequence identity with other *slpA* alleles, and has been designated SLCT-13. A partial strain 19142 *slpA* sequence was deposited in Genbank (accession: KX610658). Details of plasmid and strain construction are given in Supplementary Methods.

Bioassays to determine Avidocin-CD killing activity.

Avidocin-CD bactericidal activity was assayed by a semi-quantitative spot method as previously described (*12, 13*). For broth-based killing assays, *C. difficile* strains were grown overnight in TY broth and then sub-cultured to an OD_{600nm} of 0.05 in 1 ml fresh TY supplemented with 1mM $CaCl_2$. Av-CD291.2 (50 μl) was added to each culture after 2.5 h. Growth was monitored by measuring the OD_{600nm} hourly.

Extraction of S-layer and associated proteins.

S-layer proteins were extracted using low pH glycine as previously described (*8*) and analyzed by SDS-PAGE using standard methods.

Quantitative analysis of sporulation and germination.

Quantitative analysis of sporulation was carried out as previously described (*19*) and monitored by phase contrast and transmission electron microscopy as described in Supplementary Methods.

Analysis of resistance to lysozyme and LL-37.

Broth based killing assays were carried out as described above but with lysozyme (500 μg/ml) or LL-37 (5 μg/ml) added after 2.5 h growth. Cell density was monitored by measuring the OD_{600nm} hourly. Assays were carried out in triplicate on biological duplicates.

Animal experiments.

The Golden Syrian hamster model was performed as previously described (*39*). All procedures were performed in strict accordance with the Animals (Scientific Procedures) Act 1986 with specific approval granted by the Home Office, U.K. (PPL60/4218). Further detail is given in Supplementary Methods.

Quantification of toxin expression.

Quantification of toxin activity was performed using Vero cells as described previously (*39*) and by Western immunoblot using anti-Toxin B antibody. Further details are given in Supplementary methods.

Statistical analyses.

Data were analyzed using GraphPad Prism software (GraphPad Software Inc.). Toxin production was compared using a two-tailed nonparametric Mann-Whitney test, and animal survival curves were analyzed using a Log-rank (Mantel-Cox) test. All other statistical analyses were performed using two-tailed *t*-tests with Welch's correction.

List of Supplementary Materials

Material and Methods

Fig. S1. Restoration of wild type *slpA* to the chromosome of FM2.5 and FM2.6.

Fig. S2. *C. difficile* strain sensitivity patterns to Avidocin-CDs and Diffocin-4.

Fig. S3. Avidocin-CD sensitivity correlates with SLCT.

Fig. S4. Characterization of growth and sporulation.

Fig. S5. Spore morphology and thermal sensitivity.

Fig. S6. Bactericidal activity by Avidocin-CD does not result in intracellular toxin release.

Fig. S7. Comparison of *C. difficile* bacteriophage host range vs. Avidocin-CD sensitivity.

Fig. S8. Clustal Omega alignment of SlpA sequences from strains 630 and M68.

Fig. S9. Schematic describing Avidocin-CD construction.

Table S1. Newly identified *C. difficile* phages.

Table S2. Primers used in this study

Table S3. Genbank accession identifiers.

References

1. J. R. Marchesi, D. H. Adams, F. Fava, G. D. Hermes, G. M. Hirschfield, G. Hold, M. N. Quraishi, J. Kinross, H. Smidt, K. M. Tuohy, L. V. Thomas, E. G. Zoetendal, A. Hart, The gut microbiota and host health: a new clinical frontier. *Gut* **65**, 330-339 (2016).
2. D. A. Rasko, V. Sperandio, Anti-virulence strategies to combat bacteria-mediated disease. *Nat. Rev. Drug Discov.* **9**, 117-128 (2010).
3. R. C. Allen, R. Popat, S. P. Diggle, S. P. Brown, Targeting virulence: can we make evolution-proof drugs? *Nat. Rev. Microbiol.* **12**, 300-308 (2014).
4. F. C. Lessa , Y. Mu , W. M. Bamberg , Z. G. Beldavs , G. K. Dumyati , J. R. Dunn , M. M. Farley , S. M. Holzbauer , J. I. Meek , E. C. Phipps , L. E. Wilson , L. G. Winston , J. A. Cohen , B. M. Limbago , S. K. Fridkin , D. N. Gerding , L. C. McDonald Burden of *Clostridium difficile* Infection in the United States. *New Engl. J. Med.* **372**, 825-834 (2015).
5. "ANTIBIOTIC RESISTANCE THREATS in the United States, 2013," *Threat Report 2013* (Centers for Disease Control and Prevention, Atlanta, 2013).
6. W. K. Smits, D. Lyras, D. B. Lacy, M. H. Wilcox, E. J. Kuijper, *Clostridium difficile* infection. *Nat Rev Dis Primers* **2**, 16020 (2016).
7. R. P. Fagan, N. F. Fairweather, Biogenesis and functions of bacterial S-layers. *Nat. Rev. Microbiol.* **12**, 211-222 (2014).
8. R. P. Fagan, D. Albesa-Jove, O. Qazi, D. I. Svergun, K. A. Brown, N. F. Fairweather, Structural insights into the molecular organization of the S-layer from *Clostridium difficile*. *Mol. Microbiol.* **71**, 1308-1322 (2009).

9. K. E. Dingle, X. Didelot, M. A. Ansari, D. W. Eyre, A. Vaughan, D. Griffiths, C. L. Ip, E. M. Batty, T. Golubchik, R. Bowden, K. A. Jolley, D. W. Hood, W. N. Fawley, A. S. Walker, T. E. Peto, M. H. Wilcox, D. W. Crook, Recombinational switching of the *Clostridium difficile* S-layer and a novel glycosylation gene cluster revealed by large-scale whole-genome sequencing. *J. Infect. Dis.* **207**, 675-686 (2013).

10. S. E. Willing, T. Candela, H. A. Shaw, Z. Seager, S. Mesnage, R. P. Fagan, N. F. Fairweather, *Clostridium difficile* surface proteins are anchored to the cell wall using CWB2 motifs that recognise the anionic polymer PSII. *Mol. Microbiol.* **96**, 596-608 (2015).

11. A. Ryan, M. Lynch, S. M. Smith, S. Amu, H. J. Nel, C. E. McCoy, J. K. Dowling, E. Draper, V. O'Reilly, C. McCarthy, J. O'Brien, D. Ni Eidhin, M. J. O'Connell, B. Keogh, C. O. Morton, T. R. Rogers, P. G. Fallon, L. A. O'Neill, D. Kelleher, C. E. Loscher, A role for TLR4 in *Clostridium difficile* infection and the recognition of surface layer proteins. *PLoS Pathog* **7**, e1002076 (2011).

12. D. Gebhart, S. Lok, S. Clare, M. Tomas, M. Stares, D. Scholl, C. J. Donskey, T. D. Lawley, G. R. Govoni, A modified R-type bacteriocin specifically targeting *Clostridium difficile* prevents colonization of mice without affecting gut microbiota diversity. *mBio* **6**, e02368 (2015).

13. D. Gebhart, S. R. Williams, K. A. Bishop-Lilly, G. R. Govoni, K. M. Willner, A. Butani, S. Sozhamannan, D. Martin, L. C. Fortier, D. Scholl, Novel high-molecular-weight, R-type bacteriocins of *Clostridium difficile*. *J. Bacteriol.* **194**, 6240-6247 (2012).

14. P. Ge, D. Scholl, P. G. Leiman, X. Yu, J. F. Miller, Z. H. Zhou, Atomic structures of a bactericidal contractile nanotube in its pre- and postcontraction states. *Nat. Struct. Mol. Biol.* **22**, 377-382 (2015).

15. D. Scholl, M. Cooley, S. R. Williams, D. Gebhart, D. Martin, A. Bates, R. Mandrell, An engineered R-type pyocin is a highly specific and sensitive bactericidal agent for the food-borne pathogen *Escherichia coli* O157:H7. *Antimicrob. Agents Chemother.* **53**, 3074-3080 (2009).

16. D. Scholl, D. Gebhart, S. R. Williams, A. Bates, R. Mandrell, Genome sequence of *E. coli* O104:H4 leads to rapid development of a targeted antimicrobial agent against this emerging pathogen. *PLoS One* **7**, e33637 (2012).

17. S. R. Williams, D. Gebhart, D. W. Martin, D. Scholl, Retargeting R-type pyocins to generate novel bactericidal protein complexes. *Appl. Environ. Microbiol.* **74**, 3868-3876 (2008).

18. M. Sara, U. B. Sleytr, Molecular sieving through S layers of *Bacillus stearothermophilus* strains. *J. Bacteriol.* **169**, 4092-4098 (1987).

19. M. Dembek, L. Barquist, C. J. Boinett, A. K. Cain, M. Mayho, T. D. Lawley, N. F. Fairweather, R. P. Fagan, High-throughput analysis of gene essentiality and sporulation in *Clostridium difficile*. *mBio* **6**, e02383 (2015).

20. T. D. Ho, K. B. Williams, Y. Chen, R. F. Helm, D. L. Popham, C. D. Ellermeier, *Clostridium difficile* extracytoplasmic function sigma factor sigmaV regulates lysozyme resistance and is necessary for pathogenesis in the hamster model of infection. *Infect. Immun.* **82**, 2345-2355 (2014).

21. D. M. Bowdish, D. J. Davidson, Y. E. Lau, K. Lee, M. G. Scott, R. E. Hancock, Impact of LL-37 on anti-infective immunity. *J Leukoc Biol* **77**, 451-459 (2005).

22. L. J. Deakin, S. Clare, R. P. Fagan, L. F. Dawson, D. J. Pickard, M. R. West, B. W. Wren, N. F. Fairweather, G. Dougan, T. D. Lawley, The *Clostridium difficile spo0A* gene is a persistence and transmission factor. *Infect. Immun.* **80**, 2704-2711 (2012).

23. D. Paredes-Sabja, A. Shen, J. A. Sorg, *Clostridium difficile* spore biology: sporulation, germination, and spore structural proteins. *Trends Microbiol.* **22**, 406-416 (2014).

24. J. Barra-Carrasco, V. Olguin-Araneda, A. Plaza-Garrido, C. Miranda-Cardenas, G. Cofre-Araneda, M. Pizarro-Guajardo, M. R. Sarker, D. Paredes-Sabja, The *Clostridium difficile* exosporium cysteine (CdeC)-rich protein is required for exosporium morphogenesis and coat assembly. *J. Bacteriol.* **195**, 3863-3875 (2013).

25. P. Setlow, Spores of *Bacillus subtilis*: their resistance to and killing by radiation, heat and chemicals. *J. Appl. Microbiol.* **101**, 514-525 (2006).

26. P. C. Strong, K. M. Fulton, A. Aubry, S. Foote, S. M. Twine, S. M. Logan, Identification and characterization of glycoproteins on the spore surface of *Clostridium difficile*. *J. Bacteriol.* **196**, 2627-2637 (2014).

27. E. M. Ransom, K. B. Williams, D. S. Weiss, C. D. Ellermeier, Identification and characterization of a gene cluster required for proper rod shape, cell division, and pathogenesis in *Clostridium difficile*. *J. Bacteriol.* **196**, 2290-2300 (2014).

28. J. Y. Nale, J. Spencer, K. R. Hargreaves, A. M. Buckley, P. Trzepinski, G. R. Douce, M. R. Clokie, Bacteriophage combinations significantly reduce *Clostridium difficile* growth *in vitro* and proliferation *in vivo*. *Antimicrob. Agents Chemother.* **60**, 968-981 (2016).

29. O. Sekulovic, J. R. Garneau, A. Neron, L. C. Fortier, Characterization of temperate phages infecting *Clostridium difficile* isolates of human and animal origins. *Appl. Environ. Microbiol.* **80**, 2555-2563 (2014).

30. J. E. Samson, A. H. Magadan, M. Sabri, S. Moineau, Revenge of the phages: defeating bacterial defences. *Nat. Rev. Microbiol.* **11**, 675-687 (2013).

31. J. M. Ritchie, J. L. Greenwich, B. M. Davis, R. T. Bronson, D. Gebhart, S. R. Williams, D. Martin, D. Scholl, M. K. Waldor, An *Escherichia coli* O157-specific engineered pyocin prevents and ameliorates infection by *E. coli* O157:H7 in an animal model of diarrheal disease. *Antimicrob. Agents Chemother.* **55**, 5469-5474 (2011).

32. E. Llobet, J. M. Tomas, J. A. Bengoechea, Capsule polysaccharide is a bacterial decoy for antimicrobial peptides. *Microbiology* **154**, 3877-3886 (2008).

33. R. D. Plaut, J. W. Beaber, J. Zemansky, A. P. Kaur, M. George, B. Biswas, M. Henry, K. A. Bishop-Lilly, V. Mokashi, R. M. Hannah, R. K. Pope, T. D. Read, S. Stibitz, R. Calendar, S. Sozhamannan, Genetic evidence for the involvement of the S-layer protein gene *sap* and the sporulation genes *spo0A*, *spo0B*, and *spo0F* in Phage AP50c infection of *Bacillus anthracis*. *J. Bacteriol.* **196**, 1143-1154 (2014).

34. M. M. Merrigan, A. Venugopal, J. L. Roxas, F. Anwar, M. J. Mallozzi, B. A. Roxas, D. N. Gerding, V. K. Viswanathan, G. Vedantam, Surface-layer protein A (SlpA) is a major contributor to host-cell adherence of *Clostridium difficile*. *PLoS One* **8**, e78404 (2013).

35. J. K. Shim, S. Johnson, M. H. Samore, D. Z. Bliss, D. N. Gerding, Primary symptomless colonisation by *Clostridium difficile* and decreased risk of subsequent diarrhoea. *Lancet* **351**, 633-636 (1998).

36. B. Dupuy, A. L. Sonenshein, Regulated transcription of *Clostridium difficile* toxin genes. *Mol. Microbiol.* **27**, 107-120 (1998).

37. H. Kato, Typing by sequencing the *slpA* gene of *Clostridium difficile* strains causing multiple outbreaks in Japan. *J. Med. Microbiol.* **54**, 167-171 (2005).

38. T. Karjalainen, N. Saumier, M. C. Barc, M. Delmee, A. Collignon, *Clostridium difficile* genotyping based on *slpA* variable region in S-layer gene sequence: an alternative to serotyping. *J. Clin. Microbiol.* **40**, 2452-2458 (2002).

39. A. M. Buckley, J. Spencer, D. Candlish, J. J. Irvine, G. R. Douce, Infection of hamsters with the UK *Clostridium difficile* ribotype 027 outbreak strain R20291. *J. Med. Microbiol.* **60**, 1174-1180 (2011).

40. R. P. Fagan, N. F. Fairweather, *Clostridium difficile* has two parallel and essential Sec secretion systems. *J. Biol. Chem.* **286**, 27483-27493 (2011).

41. C. S. Wong, S. Jelacic, R. L. Habeeb, S. L. Watkins, P. I. Tarr, The risk of the hemolytic-uremic syndrome after antibiotic treatment of *Escherichia coli* O157:H7 infections. *N Engl J Med* **342**, 1930-1936 (2000).

42. J. Peltier, H. A. Shaw, E. C. Couchman, L. F. Dawson, L. Yu, J. S. Choudhary, V. Kaever, B. W. Wren, N. F. Fairweather, Cyclic diGMP regulates production of sortase substrates of *Clostridium difficile* and their surface exposure through ZmpI protease-mediated cleavage. *J. Biol. Chem.* **290**, 24453-24469 (2015).

Acknowledgments:

We thank Fred Tenover, Tom Riley, Trevor Lawley, Vince Young, and Kate Dingle for providing *C. difficile* isolates; Neil Fairweather for a plasmid containing SLCT-11 *slpA*; Hilary Browne and Trevor Lawley for providing strain CD305 genome sequence; Chris Hill and the University of Sheffield Electron Microscopy Unit for TEM analysis.

Funding:

Supported by the National Institute of Allergy and Infectious Diseases of the National Institutes of Health under Award Number R21AI121692. The content is solely the responsibility of the authors and does not necessarily represent the official views of the National Institutes of Health. Additional support from the MRC (grant number MR/N000900/1; R.P.F.), AvidBiotics Corp. and the University of Sheffield via the Higher Education Innovation Fund 2011-2015 (R.P.F.), and the Wellcome Trust (grant number 086418; G.R.D.).

Author contributions:

D.S., G.R.D., G.R.G. and R.P.F. designed and coordinated the study. J.A.K, D.G., A.M.B., S.L., G.R.G. conducted the experiments. G.R.D., G.R.G. and R.P.F. wrote the manuscript with contributions from all co-authors.

Competing interests:

D.G., S.L., D.S., and G.R.G. are current or past employees of and own stock in AvidBiotics Corp. R.P.F. received a research grant from AvidBiotics Corp. AvidBiotics Corp. hold the following patents: US8206971 (Modified bacteriocins and methods for their use), US8673291 (Diffocins and methods of use therof), US9115354 (Diffocins and methods of use therof), and EP2576604 (Diffocins and methods of use therof).

Data and materials availability:

Nucleotide sequences have been deposited in Genbank with accession identifiers: KX610658, KX557294, KX592438, KX592434, KX592441. KX592442, KX592443, KX592444, KX592439, KX592435, KX592437, KX592436, KX592440. Avidocin-CDs are available from AvidBiotics Corp. subject to a material transfer agreement.

Figure Legends:

Fig. 1. Mutations in *slpA* confer Av-CD291.2 resistance. (**A**) Alignment of the *slpA* sequence (nucleotides 268-294) from R20291, FM2.5, FM2.6, FM2.5RW and FM2.6RW. A nucleotide insertion at position 283 of FM2.5 *slpA* results in a frameshift and premature stop codon (in blue). A nucleotide substitution at position 280 of FM2.6 *slpA* results in a nonsense mutation (in red). To allow differentiation from the wild type sequence, two synonymous mutations were introduced into *slpA* in FM2.5RW and FM2.6RW (in green) (**B**) SDS-PAGE analysis of S-layer extracts from R20291, FM2.5, FM2.6, FM2.5RW and FM2.6RW. The positions of the LMW and HMW SLPs and minor cell wall proteins Cwp2 and Cwp6 are indicated. (**C and D**) The impact of Av-CD291.2 on exponentially growing R20291, FM2.5, FM2.5RW and FM2.6RW was monitored by measuring the optical density at 600 nm. Av-D291.2 addition is indicated with an arrow. Experiments were carried out in triplicate on biological duplicates. Means and standard deviations are shown. (**E**) SDS-PAGE analysis and Av-CD291.2 sensitivity of FM2.5 complemented with *slpA* alleles from multiple SLCTs following induction with anhydrotetracycline (20 ng/ml). R20291 and FM2.5RW are included as controls. A zone of clearance in the agar lawn indicates killing.

Fig. 2. Avidocin-CD sensitivity correlates with SLCT. **(A)** SDS-PAGE analysis of SLPs extracted from a panel of strains representing the 11 most commonly isolated SLCTs. **(B)** Spot bioassays with 8 Avidocin-CDs on the *C. difficile* strains used in panel A, as well as FM2.5 alone (-) and FM2.5 complemented with *slpA* alleles from 10 SLCTs following induction with anhydrotetracycline (20 ng/ml). The zone of clearance caused by each Avidocin-CD is shown along with SLCT (H = Hybrid 2/6).

Fig. 3. Phenotypic characterization of FM2.5. **(A and B)** Cultures of R20291, FM2.5 and FM2.5RW were challenged with lysozyme (500 µg/ml; **A**) or LL-37 (5 µg/ml; **B**) in exponential phase after 2.5 h (indicated with arrows). Untreated control cultures were grown in parallel. Experiments were carried out in triplicate on biological duplicates. Means and standard deviations are shown. **(C)** Sporulation of R20291, FM2.5, and FM2.5RW after 5 days. Spore CFUs were determined following a standard 65°C heat treatment for 30 minutes or a harsher 75°C heat treatment for 30 minutes. Heat-resistant spore CFUs are expressed as a percentage of total viable CFUs (spores and vegetative cells). Experiments were carried out in duplicate on biological duplicates. Mean and standard deviation are shown. * = $P<0.01$, determined using using two-tailed *t*-tests with Welch's correction. **(D)** Germination of R20291, FM2.5, and FM2.5RW spores. Synchronous germination of purified spores was induced with the bile salt taurocholate. Germination initiation was monitored by measuring the resulting decrease in optical density at OD_{600nm}.

Fig. 4. *In vivo* analysis of *slpA* mutant in the Syrian Golden hamster. (**A**) Times to experimental endpoint of animals infected with R20291 (black line), FM2.5 (dark blue line) and FM2.5RW (light blue line) respectively. Each line represents 6 animals. (**B**) Total CFUs and spore CFUs (following heat treatment at 56°C for 20 min) were determined for Lumen- (LA) and tissue-associated (TA) bacteria recovered from caecum (CAE) and colon (COL) of infected animals and quantified at experimental endpoint (R20291 and FM2.5RW) or at 14 days post-infection (FM2.5). Shown are the mean and standard error. The horizontal dotted line indicates the limit of detection. None of the observed differences, including those for the TA-spore CFUs from the

colon, are statistically significant. (**C and D**) Relative toxin activity of filtered gut samples on HT-29 (toxin A) and Vero cells (toxin B) respectively. Values represent the reciprocal of the first dilution in which cell morphology was indistinguishable from untreated wells. Samples were taken at experimental endpoint (R20291 and FM2.5RW) or at 14 days post-infection (FM2.5). (* = $P < 0.05$, ** = $P < 0.01$, NS = not significant, determined using using a two-tailed nonparametric Mann-Whitney test. **(E)** *In vitro* cell lysate and culture supernatant samples from R20291, FM2.5 and FM2.5RW were normalized to an equivalent optical density and separated on 6% SDS polyacrylamide gels. Toxin B was detected by Western immunoblot using an anti-Toxin B monoclonal antibody. Samples were taken at the indicated time points.

Fig. 5. Schematic diagram depicting the phenotypes of Wild Type **(A)** and S-layer null mutant **(B)** cells in *C. difficile* biology and pathophysiology. Processes labeled in black indicate new functions discerned in this manuscript. Processes labeled in grey indicate previously identified functions. Dotted lines indicate relationships that need to be studied further. Question marks indicate previously described connections incompatible with observations made with the S-layer null mutant and warranting further investigation. **(C)** Schematic of Avidocin-CD structure and function. Binding to *C. difficile* by the Avidocin-CD receptor binding proteins (RBPs) triggers the sheath to contract and force the hollow nanotube core across the cell envelope. The resulting pore allows small metabolites, such as protons, ATP and cations, to escape from the cell cytoplasm, which, in turn, disrupts the cell's membrane potential and kills the cell.

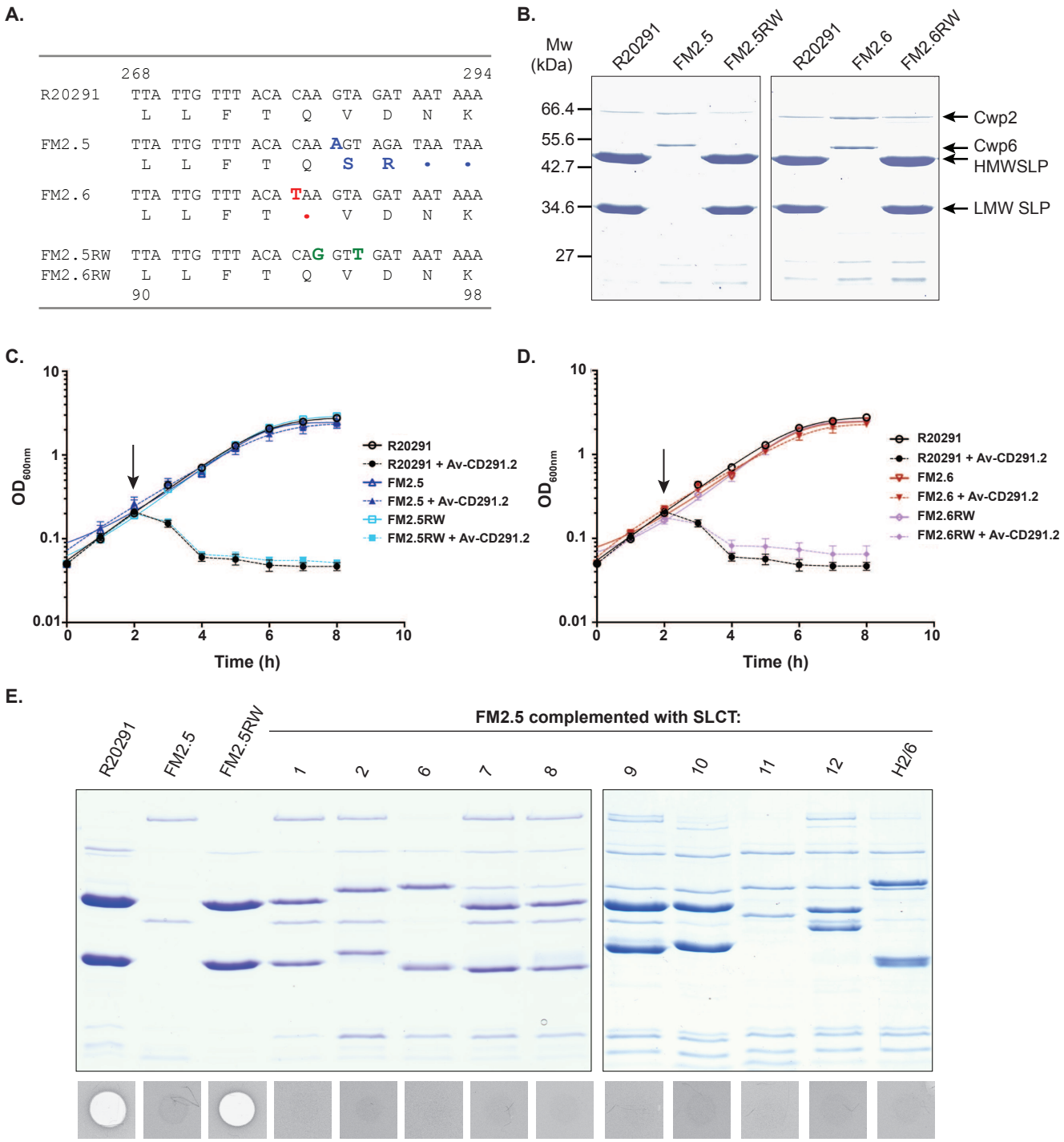
A.
268 294
R20291 TTA TTG TTT ACA CAA GTA GAT AAT AAA
L L F T Q V D N K
FM2.5 TTA TTG TTT ACA CAA AGT AGA TAA TAA
L L F T Q S R • •
FM2.6 TTA TTG TTT ACA TAA GTA GAT AAT AAA
L L F T • V D N K
FM2.5RW TTA TTG TTT ACA CAG GTT GAT AAT AAA
FM2.6RW L L F T Q V D N K
90 98
B.
Mw (kDa)
R20291
FM2.5
FM2.5RW
R20291
FM2.6
FM2.6RW
66.4
55.6
42.7
34.6
27
Cwp2
Cwp6
HMWSLP
LMW SLP
C.
OD600nm
Time (h)
R20291
R20291 + Av-CD291.2
FM2.5
FM2.5 + Av-CD291.2
FM2.5RW
FM2.5RW + Av-CD291.2
D.
OD600nm
Time (h)
R20291
R20291 + Av-CD291.2
FM2.6
FM2.6 + Av-CD291.2
FM2.6RW
FM2.6RW + Av-CD291.2
E.
FM2.5 complemented with SLCT:
R20291
FM2.5
FM2.5RW
1
2
6
7
8
9
10
11
12
H2/6

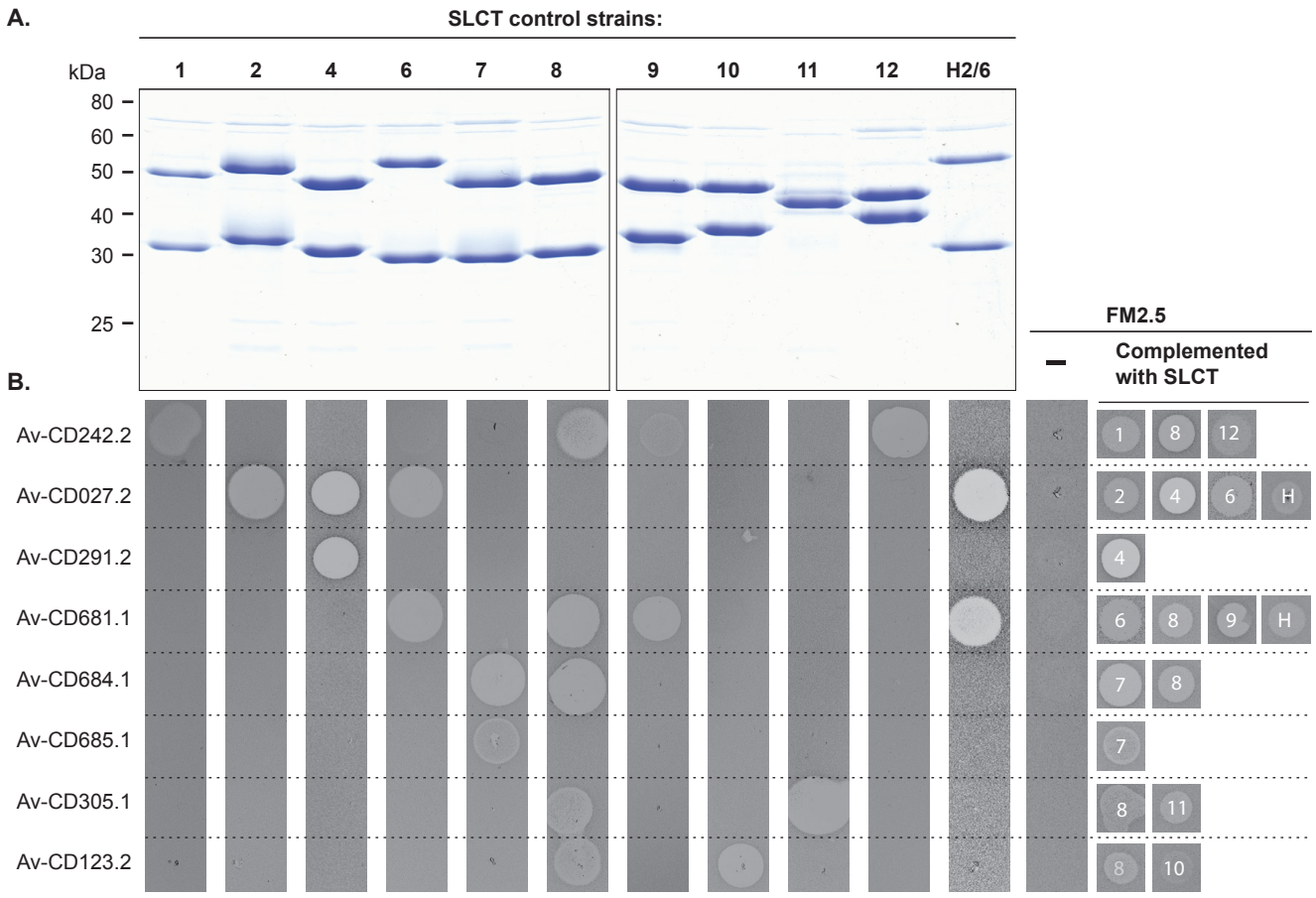
A.
SLCT control strains:
kDa
1
2
4
6
7
8
9
10
11
12
H2/6
80
60
50
40
30
25
B.
FM2.5
–
Complemented with SLCT
Av-CD242.2
Av-CD027.2
Av-CD291.2
Av-CD681.1
Av-CD684.1
Av-CD685.1
Av-CD305.1
Av-CD123.2
1 8 12
2 4 6 H
4
6 8 9 H
7 8
7
8 11
8 10

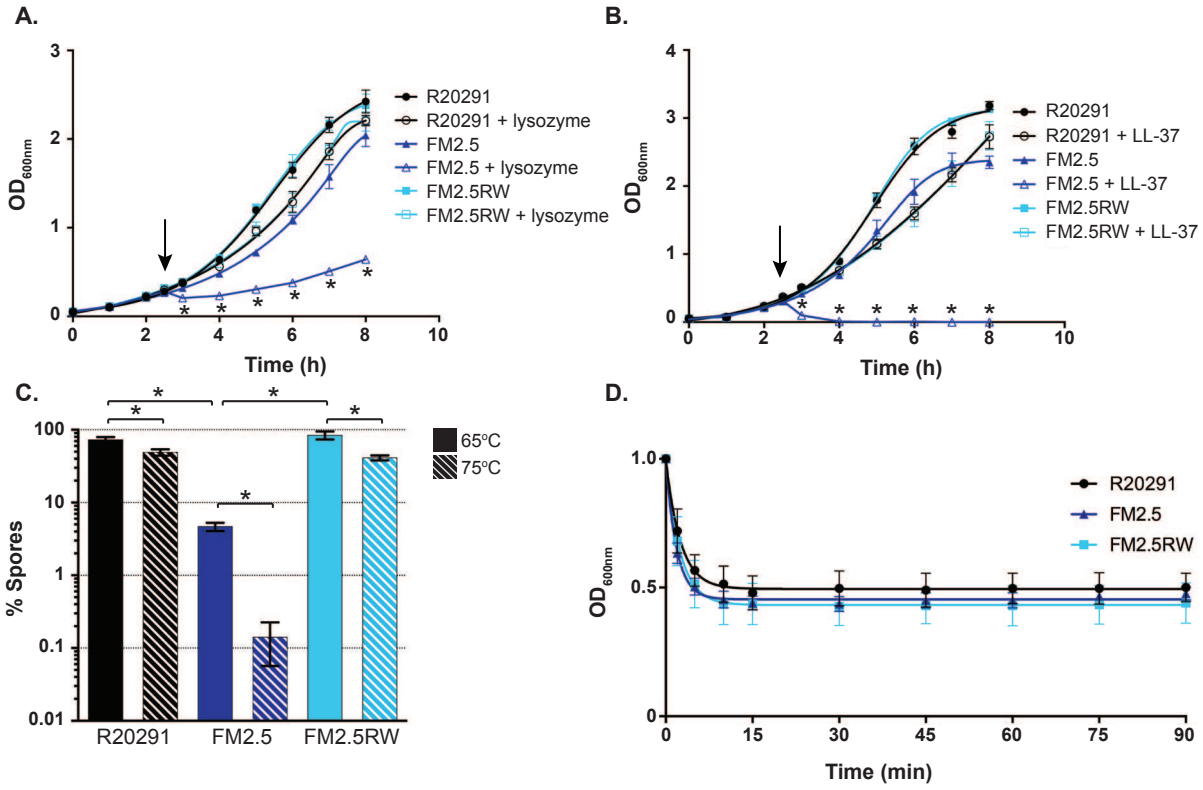
A.
OD600nm
Time (h)
R20291
R20291 + lysozyme
FM2.5
FM2.5 + lysozyme
FM2.5RW
FM2.5RW + lysozyme
B.
OD600nm
Time (h)
R20291
R20291 + LL-37
FM2.5
FM2.5 + LL-37
FM2.5RW
FM2.5RW + LL-37
C.
% Spores
65ºC
75ºC
R20291
FM2.5
FM2.5RW
D.
OD600nm
Time (min)
R20291
FM2.5
FM2.5RW

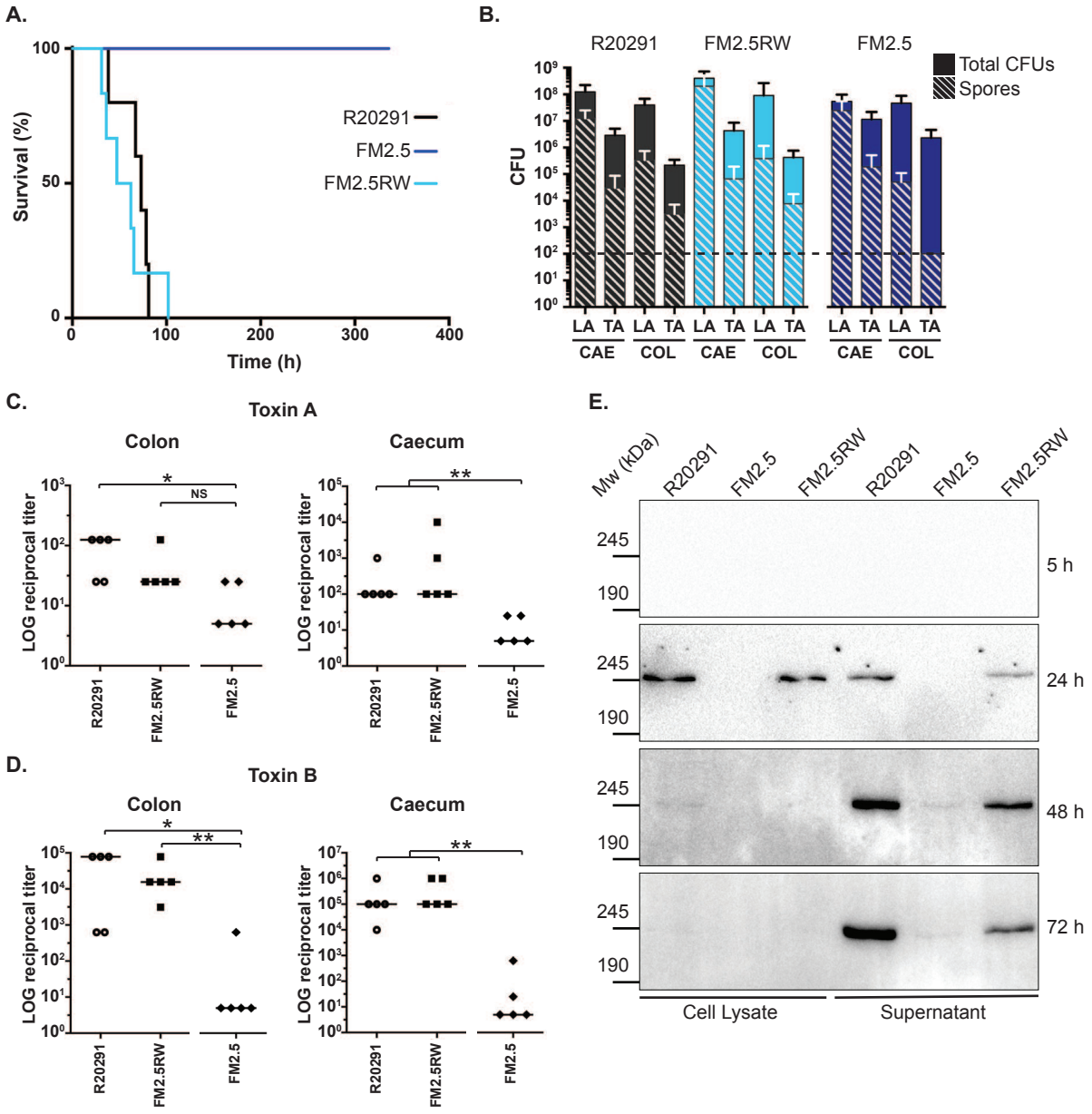
A.
Survival (%)
Time (h)
R20291
FM2.5
FM2.5RW
B.
R20291
FM2.5RW
FM2.5
Total CFUs
Spores
CFU
LA TA LA TA LA TA LA TA LA TA LA TA
CAE COL CAE COL CAE COL
C.
Toxin A
Colon
Caecum
LOG reciprocal titer
NS
D.
Toxin B
E.
Mw (kDa)
245
190
5 h
24 h
48 h
72 h
Cell Lysate
Supernatant

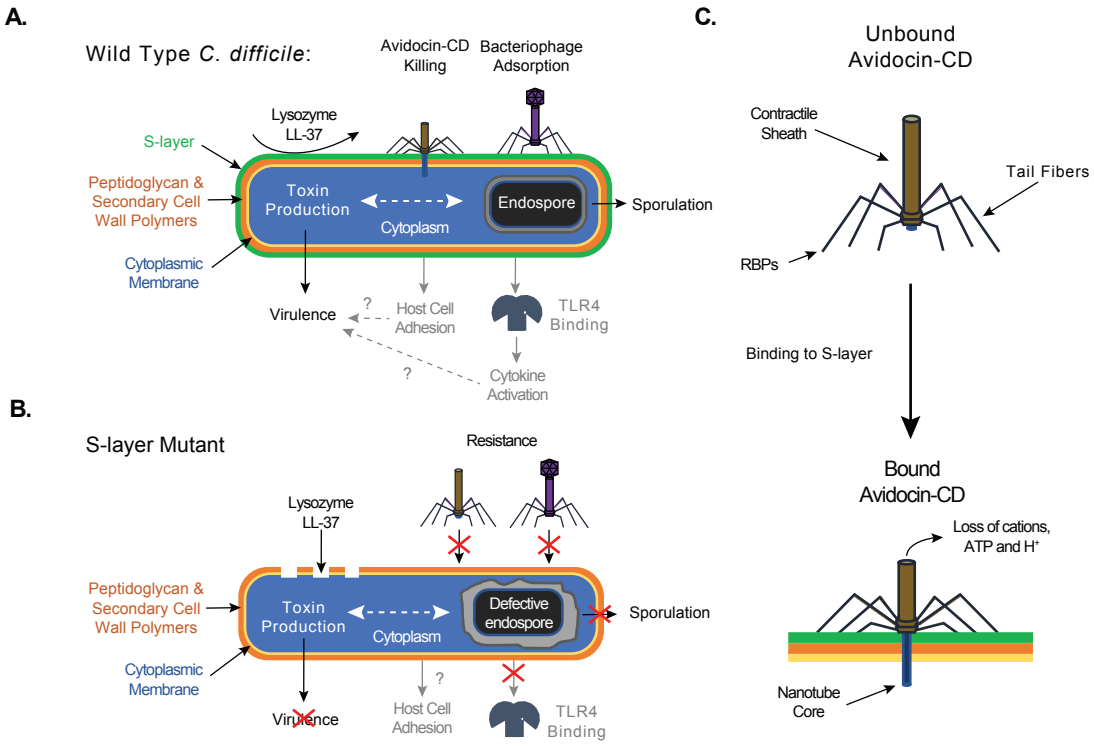
A.
Wild Type C. difficile:
Avidocin-CD Killing
Bacteriophage Adsorption
Lysozyme LL-37
S-layer
Peptidoglycan & Secondary Cell Wall Polymers
Cytoplasmic Membrane
Toxin Production
Cytoplasm
Endospore
Sporulation
Virulence
?
Host Cell Adhesion
TLR4 Binding
?
Cytokine Activation
B.
S-layer Mutant
Resistance
Lysozyme LL-37
Peptidoglycan & Secondary Cell Wall Polymers
Cytoplasmic Membrane
Toxin Production
Cytoplasm
Defective endospore
Sporulation
Virulence
?
Host Cell Adhesion
TLR4 Binding
C.
Unbound Avidocin-CD
Contractile Sheath
Tail Fibers
RBPs
Binding to S-layer
Bound Avidocin-CD
Loss of cations, ATP and H+
Nanotube Core

SUPPLEMENTAL MATERIALS

Material and Methods

Cloning of *slpA* alleles and construction of revertants.

The *slpA* genes from a panel of *C. difficile* strains with distinct SLCTs were amplified using the primers listed in Table S2 and cloned between *Bam*HI and *Sac*I sites in the inducible expression plasmid pRPF185 (*40*). Plasmids were transferred into *C. difficile* strain FM2.5 by conjugation from the *E. coli* donor CA434. For construction of *slpA* revertants, a watermark consisting of two adjacent synonymous mutations, was introduced into the SLCT-4 *slpA* using primers RF135 and RF136. Single crossover recombinant colonies were identified by an enhanced growth phenotype, and recombination was confirmed by PCR using primers RF33 and NF1323. Stable double crossover revertants were isolated following growth without selection for approximately 20 generations and confirmed by screening for plasmid loss, sequencing of the *slpA* gene, and confirmation of SLP expression by SDS-PAGE analysis (described below).

Construction and expression of Avidocin-CDs.

New Avidocin-CDs were constructed with bacteriophage RBPs identified from newly isolated bacteriophages and prophage insertions. The RBP genes along with the adjacent 3'end of the Baseplate attachment region (Bpar) and chaperone genes were cloned and inserted into an integration vector containing the Diffocin-4 gene cluster via a combination of restriction enzyme digests and Gibson assembly. The fusion sites used to replace the bacteriocin genes and integrate the bacteriophage derived genes are shown (Fig. S9). Avidocin constructs using the downstream fusion site 1 are denoted with a ".1" suffix (i.e. Av-CD681.1), while constructs using the downstream fusion site 2 are denoted with a ".2" (i.e. Av-CD027.2). The resulting integration vectors were sequence verified and transformed into the *B. subtilis* production strain as previously described (*12*). The nucleotide sequences for the Bpar fusion, RBP and downstream chaperones have been deposited in Genbank along with source information. Accession numbers are provided in Table S3. Expression of each Avidocin-CD was induced with IPTG as previously

described (*12*). Preparation of each Avidocin-CD and Diffocin-4 relied on a combination of Polyethlene-glycol-8000 precipitations and ultracentrifugation as described previously (*12*).

Isolation of Av-CD291.2-resistant clones.

A greater than 100-fold excess of active Av-CD291.2 was added to exponentially growing *C. difficile* strain R20291. After 75 min bacteria were harvested, resuspended in phosphate buffered saline (PBS), and spread on non-selective Brucella agar plates maintained under anaerobic conditions at 37°C overnight. CFU counts before and after addition of Av-CD291.2 were compared to determine resistance frequency. Resistant colonies were streaked on *C. difficile*-selective agar and Av-CD291.2-resistance was confirmed. Av-CD291.2-resistant strains FM2.5 and FM2.6 was sequenced by Illumina Miseq and identified *slpA* mutations were confirmed by Sanger sequencing.

Quantitative analysis of sporulation and germination.

Overnight bacterial cultures were diluted to 0.01 OD_{600nm} in BHI-S broth, incubated for 8 hours, diluted again to 0.0001 OD_{600nm} and grown overnight. The resulting stationary phase cultures (T=0) were then incubated for 5 days. The relative proportion of spores and vegetative cells was determined at 24 h intervals by counting total and heat-resistant (65°C for 30 min) CFUs on BHI-S agar supplemented with 0.1 % taurocholate. Assays were repeated in triplicate with biological triplicates. In order to test a range of different stress conditions, additional samples were taken on day 5 and treated at either 75°C for 30 min, 50% ethanol for 30 min or incubated aerobically for 18 h before enumerating viable spores as before. For the germination studies, spores were purified as previously described (*19*) and Ca^{2+}-DPA release and core rehydration was monitored by measuring changes in OD_{600nm} upon addition of 0.5% taurocholate.

For microscopic examination, bacterial samples were washed with PBS and fixed in 3.2% paraformaldehyde. For phase contrast microscopy, samples were mounted in 80% glycerol and visualised using a Nikon Ti Eclipse inverted microscope. For TEM, samples were additionally fixed in 3% glutaraldehyde in 0.1 M cacodylate buffer followed by 1% OsO_4, then dehydrated in

ethanol and embedded in araldite resin. Embedded samples were sectioned at 85 nm on a Leica UC6 ultramicrotome, transferred onto coated copper grids, stained with uranyl acetate and lead citrate and visualized using a FEI Tecnai BioTWIN TEM at 80 kV fitted with a Gatan MS600CW camera.

Animal experiments.

All procedures were performed in strict accordance with the Animals (Scientific Procedures) Act 1986 with specific approval granted by the Home Office, U.K. (PPL60/4218) for the experiments outlined. Briefly, 3 weeks before bacterial challenge, telemetry chips were surgically inserted by laparotomy into the peritoneal cavity of female Golden Syrian hamsters. Animals were allowed to recover from surgery before being placed in cages above transponder receiver plates that allow direct monitoring of body temperature. All animals were orally dosed with clindamycin phosphate (30 mg/kg) five days prior to challenge with 10^4 spores of either *C. difficile* R20291, FM2.5 or FM2.5RW as previously described (*39*). Six animals per group were inoculated and animals monitored carefully for onset of symptoms. Animals were culled when core body temperature dropped below 35°C.

To quantify colonization at experimental endpoint, the caecum (CAE) and colon (COL) of each animal were removed, opened longitudinally and washed thoroughly in PBS to remove unbound bacteria; these organisms were designated luminal associated organisms (LA). The washed tissue was then homogenized and subsequently recovered material contained more intimately associated organisms; designated tissue associated (TA). Total viable counts were determined by plating serial dilutions on ChromID (Biomeuriex). Spores were enumerated following heat-treatment at 56°C for 20 min. Colonies from all plates were subjected to PCR amplification of both the *slpA* gene specifically, using primers RF110 and RF111, and seven repeat regions to confirm strain identity by MVLA analysis 2 to confirm strain identity.

Quantification of toxin expression.

Quantification of toxin activity was performed using a Vero cell based cytotoxicity assay. Dilutions of filtered (0.45 μm) post-challenge gut contents were added to confluent monolayers for 24h and the end-point titer was defined as the first dilution at which Vero cell morphology was indistinguishable from untreated wells. Each experiment was performed in duplicate on two separate occasions. For measurements of toxin production *in vitro*, whole cell lysates or culture supernatants were separated by SDS-PAGE, transferred to PVDF membrane and toxin B detected by Western immunoblot using a specific mouse monoclonal antibody (MA1-7413, Thermo Fisher).

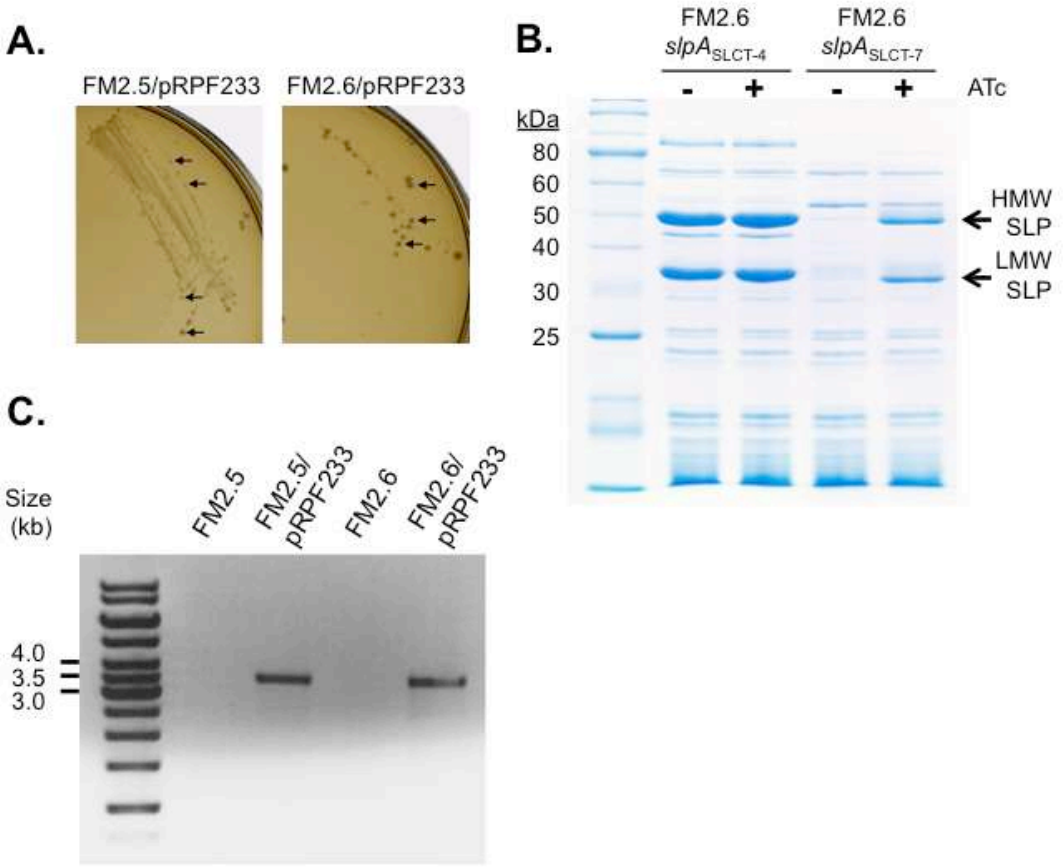

Fig. S1. Restoration of wild type *slpA* to the chromosome of FM2.5 and FM2.6. Plasmid pRPF233, carrying a wild type copy of the R20291 *slpA* gene under the control of a tetracycline-inducible promoter, was introduced into FM2.5 and FM2.6 by conjugation from an *E. coli* donor strain CA434. **(A)** When grown on solid media, supplemented with thiamphenicol to select for the plasmid, both FM2.5/pRPF233 and FM2.6/pRPF233 produced two distinct colony morphologies; small colonies that were indistinguishable from those typical of FM2.5 and FM2.6 and larger colonies that appeared to grow significantly faster than the *slpA* mutants. **(B)** When the S-layer profile of the larger colonies was analyzed by SDS-PAGE constitutive SlpA expression, independent of anhydrotetracycline (ATc) induction, was observed. However, when the *slpA* gene from strain 630 (SLCT-7), which shares 69.4% nucleotide identity with $slpA_{R20291}$ (SLCT-4), was introduced expression of SlpA remained inducible. **(C)** Analysis of these large colonies by PCR using one chromosome-specific primer (RF33, annealing 1,250 bp downstream of *slpA* in the *secA2* gene) and one plasmid-specific primer (NF1323, annealing in the P_{tet} promoter 122 bp upstream of *slpA* on pRPF233) confirmed that pRPF233 had integrated into the

chromosome at the *slpA* locus by a single crossover recombination event. Stable *slpA* revertants, FM2.5RW and FM2.6RW, were later generated from these single crossover mutants by culturing the bacteria without selection and then screening for plasmid loss and retention of the fast growth colony phenotype.

	Strain Designation	Source	Ribotype	SlpA-type	CD4 (12) RTB I Diffocin-4	R20291 (4) PI II-B Av-CD291.2	panel (4) phage II-B Av-CD027.2	M68 (7) PI II-A Av-CD681.1	M68 (7) PI II-B Av-CD682.1	M68 (7) PI/ Phage II-A Av-CD684.1	M68 (7) PI II-A Av-CD685.1	CD305 (11) PI II-A Av-CD305.1	19123 (6) phage III Av-CD123.2	CD62 (12) phage II-A Av-CD242.2	19147 (1) phage II-A Av-CD147.1	CD630 (7) PI II-A Av-CD630.1
																Strain Source (SLCT)
																RBP type
																Construct Designation
1	Ox1424 (ST12)	Dingle	003	1		-	-	-		-	-	-	-	+	+	+
2	19108	Citron	053	1	+	-	-	-		-	-	-		+	+	+
3	19147	Citron	053	1	+	-	-	-		-	-			+	+	+
4	19110	Citron	053	1	+	-	-	-		-	-		-	+	+	+
5	19098	Citron	057	1	-	-	-	-	-	-	-		-	+	+	+
			Totals (Killed/Tested)		3/4	0/5	0/5	0/5	0/1	0/5	0/5	0/2	0/3	5/5	5/5	5/5
6	Ox858 (ST16)	Dingle	029	2		-	+	-		-	-	-	-	-	-	
7	Ox2404 (ST16)	Dingle	029	2		-	+	-		-	-	-	-	-	-	
8	19117	Citron	103	2	-	-	-	-	-	-	+		-	-	-	-
9	CD843	Riley	103	2		-	-	-			+		-	-	-	-
			Totals (Killed/Tested)		0/1	0/4	2/4	0/4	0/4	0/3	2/4	0/2	0/4	0/4	0/4	0/2
10	Ox1121 (ST35)	Dingle	284	3		-	-	-		-	-	-	-	-	-	
			Totals (Killed/Tested)			0/1	0/1	0/1		0/1	0/1	0/1	0/1	0/1	0/1	
11	19103	Citron	001	4	+	+	+	-		-	-		-	-	-	
12	19135	Citron	001	4	+	+	+	-	+	-	-	-				
13	LIV24	Lawley	001	4	+	+	+	-	+	-	-					
14	BI-9	Lawley	001	4	+	+	+	-	+	-	-	-				
15	19137	Citron	015	4	+	+	+	-	+	-	-		-	-	-	
16	19129	Citron	027	4	+	+	+	-		-	-		-	-	-	
17	19139	Citron	027	4	+	+	+	-		-	-		-	-	-	
18	19126	Citron	027	4	-	+	+	-	+	-	-		-	-	-	
19	20068	Citron	027	4	-	+	+	-	+	-	-		-	-	-	
20	20315	Citron	027	4	-	+	+									
21	CD196	Lawley	027	4	-	+	+									
22	R20291	Lawley	027	4	-	+	+	-	+	-	-	-	-	-	-	-
23	Ox160 (ST1)	Dingle	027	4		+	+	-		-	-	-	-	-	-	
24	ATCC43255	ATCC	087	4	+	+	+	-	+	-	-					
			Totals (Killed/Tested)		8/13	14/14	14/14	0/12	8/8	0/12	0/12	0/4	0/8	0/8	0/8	0/1
25	Ox1437a (ST7)	Dingle	026	5		-	-	-		-	-	-	-	-	-	
			Totals (Killed/Tested)			0/1	0/1	0/1		0/1	0/1	0/1	0/1	0/1	0/1	

26	19123	Citron	014	6	-	-	+	+	+	-	-	-	-	-	-	
27	Ox1896 (ST17)	Dingle	018	6		-	+	+		-	-	-	-	-	-	
28	CD4	Fortier	024	6	w	-	+	+	+	-	-	-	-	-	-	
29	M120	Lawley	078	6H	-	-	+	+	-	-	-	-	-	-	-	
30	8119	Cepheid	078	6H			+	+								
31	8401	Cepheid	078	6H			+	+								
32	8905	Cepheid	078	6H			+	+								
33	10399	Cepheid	078	6H			+	+								
34	10411	Cepheid	078	6H			+	+								
35	Ox575 (ST11)	Dingle	078	6H		-	+	+		-	-	-	-	-	-	
				Totals (Killed/Tested)	0/2	0/4	10/10	10/10	2/3	0/5	0/5	0/5	0/5	0/5	0/5	
36	CD630	Lawley	012	7	-	-	-	-	-	+	+	-	-	-	-	-
37	M68	Lawley	017	7	+	-		-	-	+	+					
38	CF5	Lawley	017	7	+	-	-	-	-	+	+		-	-	-	
39	19119	Citron	019	7	+	-	-	-	-	+	+		-	-	-	
40	19121	Citron	019	7	+	-		-	-	+	+					
41	19134	Citron	137	7	-	-		-	-	+	+	-				
42	Ox1145 (ST4)	Dingle	137	7		-	-	-		+	+	-	-	-	-	
				Totals (Killed/Tested)	4/6	0/7	0/4	0/7	0/6	7/7	7/7	0/3	0/4	0/4	0/4	0/1
43	Ox1396 (ST54)	Dingle	012	8		+	-	+		+	-	+	+	+	-	
				Totals (Killed/Tested)		1/1	0/1	1/1		1/1	0/1	1/1	1/1	1/1	0/1	
44	19099	Citron	002	9	-	-		+	-	-	-	-				
45	19131	Citron	002	9	-			+	-	-	-					
46	TL178	Lawley	002	9	-	-		+	-	-	-	-				
47	Ox1192c (ST8)	Dingle	002	9		-	-	+		-	-	-	-	-	-	
48	TL174	Lawley	015	9	+			+	-	-	-	-				
49	19145	Citron	153	9	-	-		+	-	-	-		-	-	-	
				Totals (Killed/Tested)	1/5	0/4	0/1	6/6	0/5	0/6	0/6	0/4	0/2	0/2	0/2	
50	TL176	Lawley	014	10	-	-		-	-	-	-	-	+			-
51	19102	Citron	106	10	-			-	-	-	-		+			
52	LIV22	Lawley	106	10	-			-	-	-	-	-	+			
53	Ox1533 (ST13)	Dingle	129	10		-	-	-		-	-	-	+	-	-	
				Totals (Killed/Tested)	0/3	0/2	0/1	0/4	0/3	0/4	0/4	0/3	4/4	0/1	0/1	0/1
54	CD305	Lawley	023	11	-	-				-	-	+				
55	Ox1523 (ST5)	Dingle	023	11		-	-	-		-	-	+	-	-	-	
56	19155	Citron	080	11	-			-	-	-	-	+				
				Totals (Killed/Tested)	0/2	0/2	0/1	0/2	0/1	0/3	0/3	3/3	0/1	0/1	0/1	
57	19146	Citron	010	12	-									+		
58	CD62	Riley	010	12	-	-	-	-	-	-	-	-	-	+	-	-
59	CD242	Riley	010	12		-	-	-	-	-	-	-	-	+	-	
60	Ox1342 (ST15)	Dingle	012	12		-	-	-		-	-	-	-	+	-	
61	F200	Young	12w	12				-	-	-	-			+		
				Totals (Killed/Tested)	0/2	0/3	0/3	0/4	0/3	0/4	0/4	0/3	0/3	5/5	0/3	0/1
62	19142	Citron	046	13	-	+	-	-	-	-	-	-	-	-	-	-
				Totals (Killed/Tested)	0/1	1/1	0/1	0/1	0/1	0/1	0/1	0/1	0/1	0/1	0/1	0/1

Figure S2. *C. difficile* strain sensitivity patterns to Avidocin-CDs and Diffocin-4. Preparations of each Avidocin-CD and Diffocin-4 were serially diluted and spotted on bacterial lawns for each strain. If a zone of clearance correlating with killing was detected, the strain was deemed sensitive to the agent tested and is demarked by a "+" in the figure. If no zone of clearance was observed, the strain was deemed insensitive and is demarked with "-" in the figure. Faint zones of clearance are demarked with a "w". Not all strains were tested against each Avidocin-CD preparation. The number of strains killed per the total number of strains assayed is listed for each SLCT. Totals in red indicate less than 100% sensitivity. Boxes highlighted in red indicate testing on RBP strain source. The strain designation, source, ribotype and SLCT are listed. Source designations: Dingle = Kate Dingle, University of Oxford; Riley = Tom Riley, University of Western Australia; Lawley = Trevor Lawley, Wellcome Trust Sanger Institute; Tenover = Fred Tenover, Cepheid; Young = Vincent Young, University of Michigan; R.M.A.R. = R.M. Alden Research Laboratory.

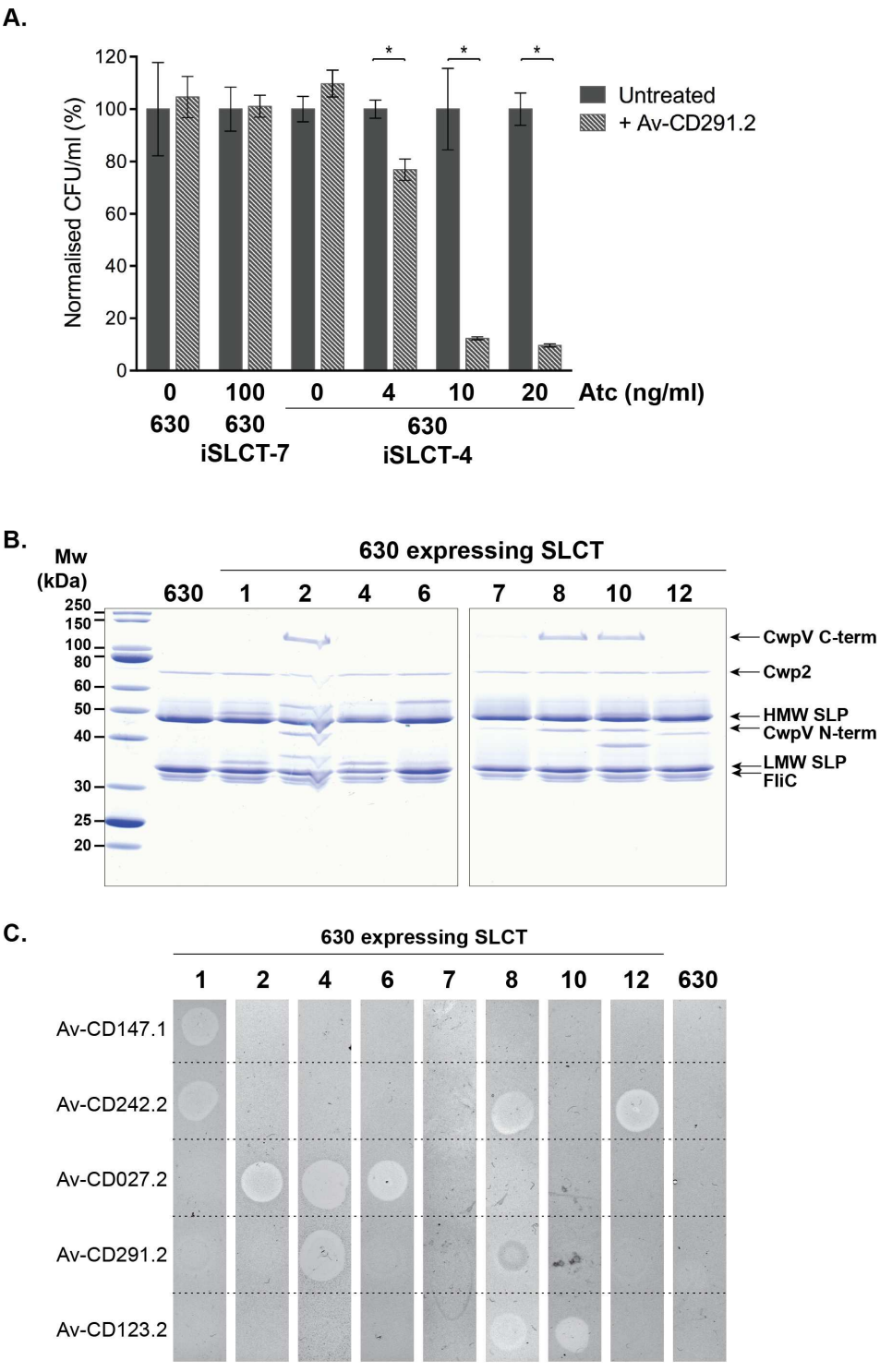

Figure S3. Avidocin-CD sensitivity correlates with SLCT. **(A)** Av-CD291.2 killing efficiency is dependent on the level of SLCT-4 SlpA induction. Strain 630 (SLCT-7) or 630 carrying a plasmid-borne inducible copy of SLCT-7 SlpA or SLCT-4 SlpA were subcultured to an OD_{600nm}

of 0.05, grown for two hours, induced with the indicated concentration of anydrotetracycline (ATc) and then challenged with Av-CD291.2 following two hours of induction. Identical untreated cultures were included as controls. Shown are means and standard deviations of biological duplicates assayed in triplicate. p =<0.01, determined using using two-tailed *t*-tests with Welch's correction. **(B)** SDS-PAGE analysis of S-layer extracts from 630 (SLCT-7) and a panel of eight 630 derivative strains expressing SLCT-1, 2, 4, 6, 7, 8, 10 and 12 under the control of a tetracycline-inducible promoter (*40*). Heterologous SlpA expression was induced with 20 ng/ml anhydrotetracycline. The positions of the LMW and HMW SLPs, the minor cell wall proteins CwpV and Cwp2, and the flagellar subunit FliC are indicated. **(C)** Spot bioassays with 5 Avidocin-CDs on the *C. difficile* strains used in panel B following induction with anhydrotetracycline (20 ng/ml). The zone of clearance caused by each Avidocin-CD is shown along with the SLCT.

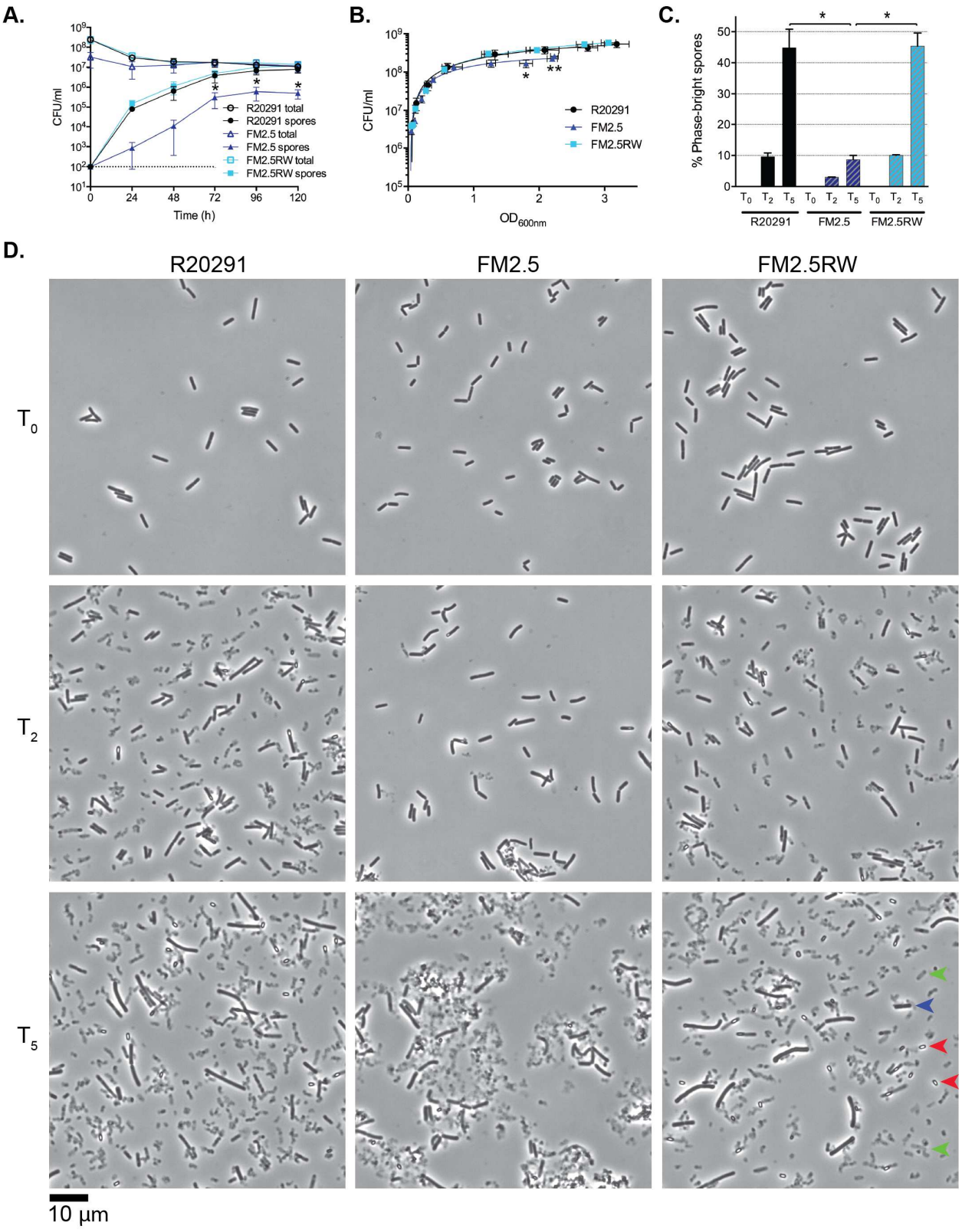
A.
CFU/ml
Time (h)
R20291 total
R20291 spores
FM2.5 total
FM2.5 spores
FM2.5RW total
FM2.5RW spores
B.
CFU/ml
OD600nm
R20291
FM2.5
FM2.5RW
C.
% Phase-bright spores
R20291
FM2.5
FM2.5RW
D.
R20291
FM2.5
FM2.5RW
T0
T2
T5
10 µm

Figure S4. Characterization of growth and sporulation. **(A)** Sporulation of R20291, FM2.5, and FM2.5RW over 5 days. Total CFUs and heat-resistant spore CFUs (65°C for 30 min) were determined at 24 h intervals. Experiments were carried out in duplicate on biological duplicates. Mean and standard deviation are shown. The dotted line indicates the limit of detection. **(B)** Overnight cultures of strains R20291, FM2.5, and FM2.5RW were subcultured to an OD_{600nm} of 0.05 and growth was monitored hourly for 9 hours by measuring the OD_{600nm} and direct counting of CFUs. Shown are the means and standard deviations of biological duplicates with technical triplicates. Growth of all 3 strains is identical until an OD_{600nm} of 1.25. FM2.5 prematurely enters stationary phase, reaching a maximum OD_{600nm} of 2.2 compared with 3.2 for R20291. **(C)** Sporulation of R20291, FM2.5, and FM2.5RW was monitored by direct counting vegetative cells and phase bright spores by phase contrast microscopy at T=0, 48 and 120 of a standard 5 day sporulation assay. 20 microscope fields were counted for each strain at each timepoint. The number of spores is expressed as a percentage of total with the mean and standard deviations shown. * = $p<0.01$, determined using using two-tailed *t*-tests with Welch's correction. **(D)** Example microscope fields representative of those counted for panel C. For clarity only 40% of each field is shown. In the bottom right image representative spores are marked with red arrow heads, a representative vegetative cell with a blue arrow head and representative cell debris with green arrow heads.

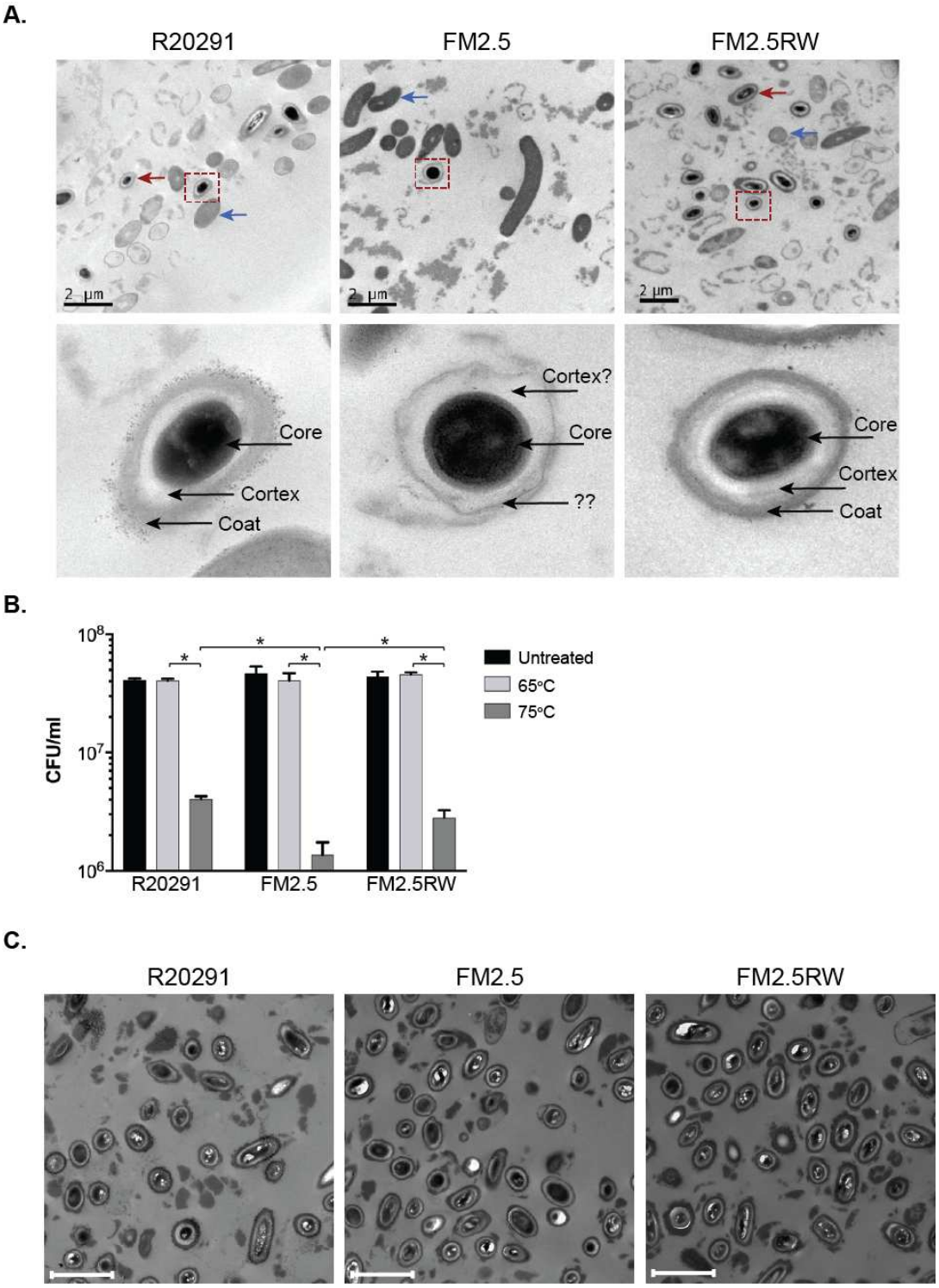

Figure S5. Spore morphology and thermal sensitivity. (**A)** Electron micrographs of cultures on day 5 of the sporulation assay shown in Figure S4A. Spore-containing representative fields are shown. Example spores (red arrows) and vegetative cells (blue arrows) are indicated. Higher magnification views of individual spores are shown below (boxed in top panels). The core,

cortex and coat layers are indicated. **(B)** Spores were purified on a 20-50% Histodenz gradient and CFUs were quantified prior to (Untreated) and following heat stress at 65°C or 75°C for 30 min. Shown are the mean and standard errors of biological triplicates assayed in triplicate. * = $p<0.01$, determined using using two-tailed *t*-tests with Welch's correction. **(C)** Electron micrographs of spores used in panel B. The scale bar on each image indicates 2 μm.

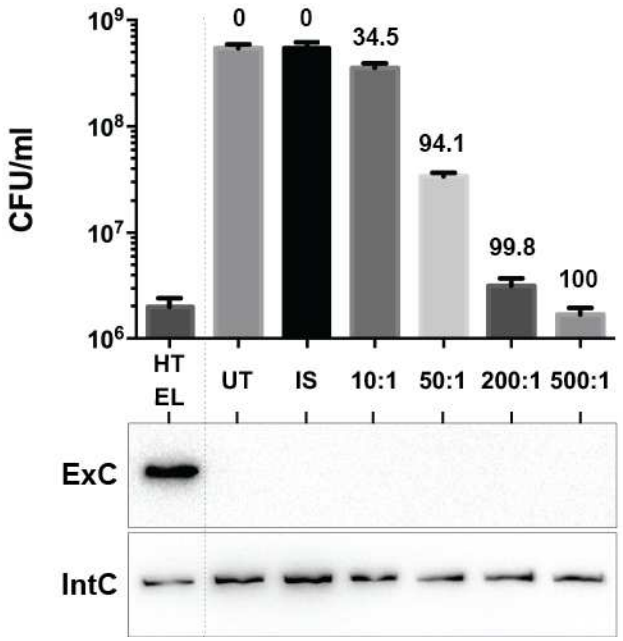

Figure S6. Bactericidal activity by Avidocin-CD does not result in intracellular toxin release. For toxin producing pathogens, antibiotics that lyse bacteria or increase toxin production can exacerbate disease severity and lessen the effectiveness of the treatment by inadvertently releasing toxins (*41*). We examined culture supernatants following treatment with Avidocin-CDs for the presence of extracellular Toxin B to determine if killing by an Avidocin-CD could result in unwanted toxin release. (A) R20291 (RT027) bacteria were incubated for an hour with either Av-CD291.2 at the indicated ratio of agent to cells, Av-CD684.1 (which does not kill strain R20291) at a 500:1 ratio, or left untreated. After incubation, surviving bacteria (CFU/mL) were enumerated. The percentage of CFU following each treatment relative to untreated control is shown. The number of spores present in the untreated sample was determined following heat treatment at 65 °C for 30 min to kill vegetative cells (lane HK). Av-CD291.2 killing occurred in a dose-dependent manner, while Av-CD684.1 treated cells behaved like untreated controls. (B) Following Avidocin-CD treatment released toxin B in culture supernatants (ExC) was detected by Western immunoblot using a specific monoclonal antibody. As a positive control for toxin release, R20291 was treated with a bacteriophage (CD27L) endolysin, which effectively lyses *C. difficile* (*42*). (C) Following Avidocin-CD treatment, the amount of remaining intracellular toxin B was determined by lysing cells with CD27L endolysin and detection by Western immunoblot as before (IntC). A fresh sample of untreated R20291 was lysed with CD27L endolysin to show

normal intracellular toxin quantities (lane EL). Despite effective killing, intracellular Toxin B remained constant with no detectable release observed in the culture supernatants (ExC) at any concentration, including samples that exhibited total killing of all vegetative bacterial cells due to a large excess (500:1) of Avidocin-CD to bacteria. These results confirm that Avidocin-CDs are bactericidal but neither lyse the target cell nor release harmful intracellular stores of toxin B. As a result, the use of Avidocin-CD to treat or prevent CDI is unlikely to exacerbate disease symptoms.

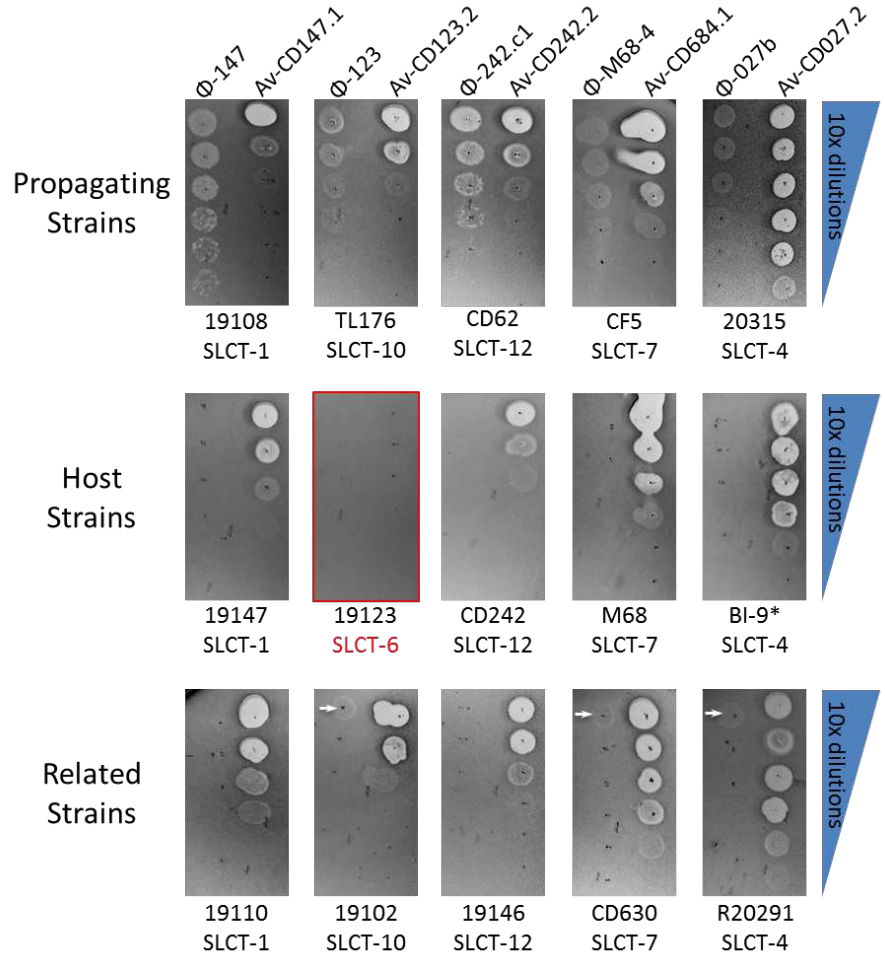

Figure S7. Comparison of *C. difficile* bacteriophage host range vs. Avidocin-CD sensitivity. Preparations of each bacteriophage and corresponding Avidocin-CD were serially diluted and spotted on bacterial lawns corresponding to the bacteriophage propagating strains, bacteriophage host strains and strains with same SLCT as propagating strain. Bacteriophage plaques are small and numerous. Avidocin-CD killing results in a large zone of clearance. Only one host strain, denoted in red, had a different SLCT than propagating strain. At high bacteriophage titers, bacteriophage are observed to cause "lysis from without" and is denoted by small white arrows.

```
SlpA-CD630      MNKKNIAIAMSGLTVLASAAPVFAATTGTQGYTVVKNDWKKAVKQLQDGLKDNSIGKITV    60
SlpA_M68        MNKKNLAMAMAAVTVVGSAAPIFADS-TTPGYTVVKNDWKKAVKQLQDGLKNKTISTIKV    59
                *****:*:**:.:**:.****:** :  * **********************:::*..*.*

SlpA-CD630      SFNDGVVGEVAPKSA-NKKADRDAAAEKLYNLVNTQLDKLGDGDYVDFSVDYNLENKIIT    119
SlpA_M68        SFNGNSVGEVTPASSGAKKADRDAAAEKLYNLVNTQLDKLGDGDYVDFEVTYNLATQIIT    119
                ***   ****:* *:  ******************************.* *** .:***

SlpA-CD630      NQADAEAIVTKLNSLNEKTLIDIATKDTFGMVSKTQDSEGKNVAATKALKVKDVATFGLK    179
SlpA_M68        K-AEAEAVLTKLQQYNDKVLINSATDTVKGMVSDTQVDSK-N-VAANPLKVSDMYTIPSA    176
                : *:***::***:. *:*.**: **. . ****.** ..  * .*:: ***.*: *:

SlpA-CD630      SGGSEDTGYVVEMKA-GAVEDKYGKVGDSTAGIAINLPST-GLEYAGKGTTIDFNKTLKV    237
SlpA_M68        ITGSDDSGYSIAKPTEKTTSLLYGTVGDATAGKAITVDTASNEAFAGNGKVIDYNKSFKA    236
                  **:*:** :   :  :..  **.***:*** **.: ::    :**:*..**:**::*.

SlpA-CD630      DVTGGSTPSAVAVSGFVTKDDTDLAKSGTINVRVINAKEESIDIDASSYTSAENLAKRYV    297
SlpA_M68        TVQGDGT---VKTSGVVLKDASDMAATGTIKVRVTSAKEESIDVDSSSYISAENLAKKYV    293
                 * * .*   * .**.* ** :*:* :***:*** .*******:*:*** *******:**

SlpA-CD630      FDPDEISEAYKAIVALQNDGIESNLVQLVNGKYQVIFYPEGKRLETKSANDTIASQDTPA    357
SlpA_M68        FNPKEVSEAYNAIVALQNDGIESDLVQLVNGKYQVIFYPEGKRLETKSA-DIIADADSPA    352
                *:*.*:****:************:************************ * **. *:**

SlpA-CD630      KVVIKANKLKDLKDYVDDLKTYNNTYSNVVTVAGEDRIETAIELSSKYYNSDDKNAITDK    417
SlpA_M68        KITIKANKLKDLKDYVDDLKTYNNTYSNVVTVAGEDRIETAIELSSKYYNSDDKNAITDD    412
                *:.*****************************************************.

SlpA-CD630      AVNDIVLVGSTSIVDGLVASPLASEKTAPLLLTSKDKLDSSVKSEIKRVMNLKSDTGINT    477
SlpA_M68        AVNNIVLVGSTSIVDGLVASPLASEKTAPLLLTSKDKLDSSVKSEIKRVMNLKSDTGINT    472
                ***:*************************************************************

SlpA-CD630      SKKVYLAGGVNSISKDVENELKNMGLKVTRLSGEDRYETSLAIADEIGLDNDKAFVVGGT    537
SlpA_M68        SKKVYLAGGVNSISKDVENELKNMGLKVTRLSGEDRYETSLAIADEIGLDNDKAFVVGGT    532
                ************************************************************

SlpA-CD630      GLADAMSIAPVASQLKDGDATPIVVVDGKAKEISDDAKSFLGTSDVDIIGGKNSVSKEIE    597
SlpA_M68        GLADAMSIAPVASQLKDGDATPIVVVDGKAKEISDDAKSFLGTSDVDIIGGKNSVSKEIE    592
                ************************************************************

SlpA-CD630      ESIDSATGKTPDRISGDDRQATNAEVLKEDDYFTDGEVVNYFVAKDGSTKEDQLVDALAA    657
SlpA_M68        ESIDSATGKTPDRISGDDRQATNAEVLKEDDYFKDGEVVNYFVAKDGSTKEDQLVDALAA    652
                *********************************.**************************

SlpA-CD630      APIAGRFKESPAPIILATDTLSSDQNVAVSKAVPKDGGTNLVQVGKGIASSVINKMKDLL    717
SlpA_M68        APIAGRFKESPAPIILATDTLSSDQNVAVSKAVPKDGGTNLVQVGKGIASSVINKMKDLL    712
                ************************************************************

SlpA-CD630      DM      719
SlpA_M68        DM      714
                **
```

Figure S8. Clustal Omega alignment of SlpA sequences from strains 630 and M68. Identical residues are demarked with an asterisk. Residues with strongly similar properties are demarked with colon. Residues with weakly similar properties are demarked with a period. An 81.7% sequence identity was found between the two SLCT-7 SlpA variants.

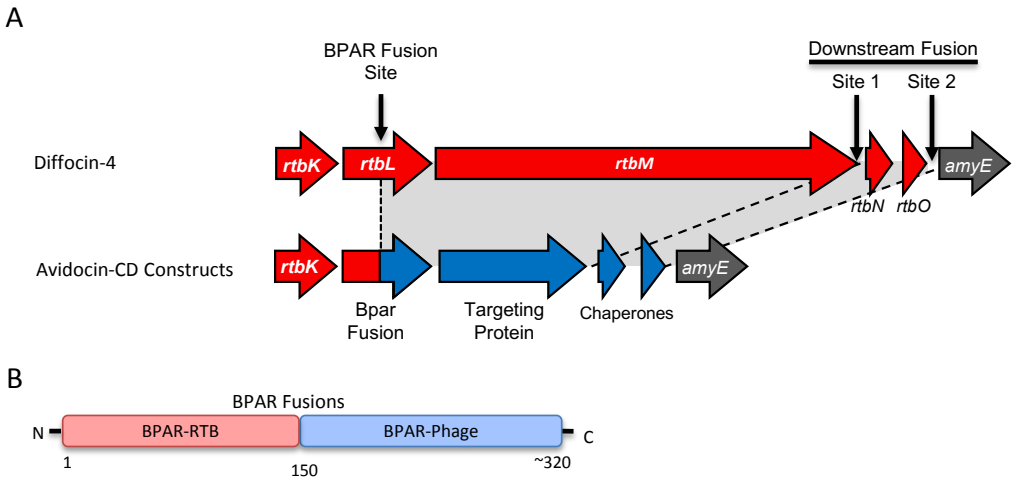

Figure S9. Schematic describing Avidocin-CD construction. (**A**) The fusion sites used to integrate the bacteriophage and prophage genes into the Diffocin-4 gene cluster are shown. There is a Bpar fusion site in *rtbL* as well as alternative downstream fusion sites before or after the predicted Diffocin-4 chaperones. The nucleotide sequences for the fusion region created in each Avidocin-CD construct fusion have been deposited in Genbank and given the following accession numbers (Table S3). (**B**) Schematic depicting R-type Bacteriocin and Bacteriophage regions for fused BPAR protein.

Table S1: Newly identified *C. difficile* phages.

Phage	Source	Propagating Strain	PtsM-like RBP
Phi-027b	panel of 027 strains	20315 (SLCT-4)	Yes
Phi-123	19123 (SLCT-6)	TL176 (SLCT-10)	No
Phi-147	19147 (SLCT-1)	19108 (SLCT-1)	Yes
Phi-242.c1	CD242 (SLCT-12)	CD62 (SLCT-12)	Yes
Phi-68.4	M68 (SLCT-7)	CF-5 (SLCT-7)	Yes

Table S2: Primers used in this study

Primer name	Primer sequence	Use
023-F	ATGAAAAAAAGAAATTTAGCA	Amplification of *slpA* variable region
023_010-R	CTATAGCTGTTTSTATTCTGTC	Amplification of *slpA* variable region
014+++-F	ATGAATAAGAAAARTTTRGCA	Amplification of *slpA* variable region
014_002+-R	CTATWGCAGTCTCTATTCTATC	Amplification of *slpA* variable region
RF1	GATCGGATCCTTACATACTTAATAAATC TTTTAATTTATTTATAACTG	Cloning of SLCT-4 *slpA* from strain R20291 with RF2
RF2	GATCGAGCTCTATAATGTTGGGAGGAAT TTAAGAAATG	Cloning of SLCT-4 *slpA* from strain R20291 with RF1
RF6	GATCGGATCCTTACATATCTAATAAATC TTTTATTTTACTTACAAC	Cloning of SLCT-H2/6 *slpA* from strain Ox575 with RF2
RF7	GATCGGATCCCTACATATCTAATAAGTC TTTTATCTTAGTG	Cloning of SLCT-10 *slpA* from strain Ox1533 with RF2
RF8	GATCGGATCCTTACATATCTAATAAATC TTTTAATTTGCTAACAAC	Cloning of SLCT-1 *slpA* from strain Ox1424 with RF2
RF33	GGCTTCTATAGCTTGGTGAA	Confirmation of *slpA* recombination with NF1323. Chromosome-specific
RF99	GATCGGATCCTTACATATCTAATAAATC TTTTATTTTATTTATTACTG	Cloning of SLCT-6 *slpA* from strain Ox1896 with RF2
RF101	GATCGGATCCTTATAATTCTAATAAATC TTTTATTCTCTTAATAAC	Cloning of SLCT-9 *slpA* from strain Ox1192c with RF134
RF110	GACATAACTGCAGCACTACTTG	Amplification of SLCT-4 *slpA* region containing point mutations and watermark
RF111	CAGGATTAACAGTATTAGCTTCTGC	Amplification of SLCT-4 *slpA* region containing point

		mutations and watermark
RF132	GATCGGATCCTTACATATTTAATAAATC TTTAAGCTTAGTTAC	Cloning of SLCT-8 *slpA* from strain Ox1396 with RF2
RF133	GATCGGATCCTTACATTCCTAATAAATC TTTTAATTTATTAATAAC	Cloning of SLCT-12 *slpA* from strain Ox1342 with RF134
RF134	GATCGAGCTCTATAATGTTGGGAGGAAT TTAAGGAATG	Cloning of SLCT-9 and 12 *slpA* with RF101 and RF133 respectively
RF135	CAGGTTGATAATAAATTAGACAATTTAG GTGATGG	Introduction of *slpA* watermark with RF136
RF136	TGTAAACAATAATTTACTTGCATCTTCT G	Introduction of *slpA* watermark with RF135
RF231	GATCGGATCCTTACATATCTAATAAATC TTTCATTTTGCTTATTAC	Cloning of SLCT-2 *slpA* from strain Ox858 with RF2
NF1323	CTGGACTTCATGAAAAACTAAAAAAAA TATTG	Confirmation of *slpA* recombination with RF33. Plasmid-specific
NF1414	GATCGAGCTCTATAATGTTGGGAGGAAT TTAAGAAATG	Cloning of SLCT-7 *slpA* from strain 630 with NF1415
NF1415	GATCGGATCCTTACATATCTAATAAATC TTTCATTTTG	Cloning of SLCT-7 *slpA* from strain 630 with NF1414

Table S3: Genbank accession identifiers.

Construct	**Source**	**Accession Id:**
Diffocin-4	CD4	KX557294
Av-CD291.2	R20291 genome	KX592438
Av-CD027.2	Phi-027b	KX592434
Av-CD681.1	M68 genome	KX592441
Av-CD682.1	M68 genome	KX592442
Av-CD684.1	M68 genome/phi-M68.4	KX592443
Av-CD685.1	M68 genome	KX592444
Av-CD305.1	CD305 genome	KX592439
Av-CD123.2	Phi-123	KX592435
Av-CD242.2	Phi-242.c1	KX592437
Av-CD147.1	Phi-147	KX592436
Av-CD630.1	630 genome	KX592440